SYNTHESIS, CHARACTERIZATION AND EVALUATION OF (CO)MoS_2 HDS SUPPORTED ON HOLLOW CARBON SPHERE FOR DESULFURIZATION OF THIOPHENE

BY

ABDULLAH FAISAL AL-AHMADI

A Thesis Presented to the
DEANSHIP OF GRADUATE STUDIES

KING FAHD UNIVERSITY OF PETROLEUM & MINERALS

DHAHRAN, SAUDI ARABIA

In Partial Fulfillment of the
Requirements for the Degree of

MASTER OF SCIENCE

In

CHEMISTRY

MAY 2013

KING FAHD UNIVERSITY OF PETROLEUM & MINERALS

DHAHRAN- 31261, SAUDI ARABIA

DEANSHIP OF GRADUATE STUDIES

This thesis, written by **Mr. Abdullah Faisal Al-Ahmadi** under the direction his thesis advisor and approved by his thesis committee, has been presented and accepted by the Dean of Graduate Studies, in partial fulfillment of the requirements for the degree of **MASTER OF SCIENCE IN CHEMISTRY.**

Dr. Mohammed A. Al-Daous
(Advisor)

Dr. Abdullah J. Al-Hamdan
Department Chairman

Dr. Mohammed Ali Morsy
(Member)

Dr. Salam A. Zummo
Dean of Graduate Studies

Dr. Oki Muraza
(Member)

12/11/13
Date

ABDULLAH FAISAL AL-AHMADI

2013

Dedication

To

My beloved family for their prayers and support and to my thesis advisor Dr. Mohammed Al-Daous

ACKNOWLEDGMENTS

First of All, All thanks to Allah for favors in helping me to complete this thesis.

My deep appreciation and acknowledgments goes to thesis committee Dr. Mohammed Abdulmajeed Al-Daous for his gaudiness and tremendous support in carrying this work.

Many thanks to Dr.Mohammed Ali Morsy and Dr. Oki Muraza for their help and comments that improved the thesis work.

I would like to thanks the center of research excellence in nano technology (CENT) for providing analytical support in electron microscopy. Special thanks to Dr.Abbas Hakeem from CENT for his dedication, support, and valuable comments that influence the research work. Also I would like to thanks Dr. Khalid AL-Majnoni from Saudi Aramco for providing us with analytical support.

I would like to thanks my family for their support and assistant that allowed me to concentrate on the research work.

Finally I would like to thanks King Fahd University of Petroleum and Minerals and chemistry department for providing me with the opportunity to study master degree in chemistry. I would also like to acknowledge King Abdulaziz City for Science and Technology (KACST) for the support provided through the Science and Technology Unit at King Fahd University of Petroleum and Minerals (KFUPM) for funding the work through project No. 10-PET1394-04 as part of the National Science, Technology and Innovation Plan.

TABLE OF CONTENTS

ACKNOWLEDGMENTS V

TABLE OF CONTENTS VI

LIST OF TABLES IX

LIST OF FIGURES X

LIST OF ABBREVIATIONS XI

ABSTRACT XIII

ملخص الرسالة XIV

CHAPTER 1 1

INTRODUCTION 1

1.1 Research Objectives: 3

2 CHAPTER 2 LITERATURE REVIEW 4

2.1 Review of Hydrodesulfurization Catalysis Technologies: 4

2.2 Sulfur Impurities in FCC Gasoline: 5

2.3 HDS Reactivity of Sulfur Compounds: 7

2.4 Mechanism of HDS reactions: 8

2.5 Supported Catalysts: 10

2.6 Carbon Support: 11

2.6.1 Poly Methyl Methacrylate Latex Templates: 11

2.6.2Tailoring the Diameter of the Product: 11

2.6.3 Carbon Spheres: 12

CHAPTER 3 EXPERIMENTAL 14

3.1 Synthesis of Polymethylmethacrylate (PMMA) Dispersion: **14**
3.1.1 Apparatus: 14
3.1.2 Synthesis: 14

3.2 Synthesis of Carbon Latex Using Resorcinol- Formaldehyde Resin: **17**

3.3 Synthesis of Molybdenum Sulfide MoS_2/C-Oxide: **17**

3.4 Synthesis of Molybdenum sulfide MoS_2 /C-Citrate: **18**

3.5 Synthesis of Cobalt promoted Molybdenum sulfide $CoMoS_2$ /C-Citrate: **18**

3.6 Synthesis of Cobalt promoted Molybdenum sulfide $CoMoS_2$ /C-Oxide: **19**

3.7 Synthesis of Cobalt promoted Molybdenum sulfide $CoMoS_2$ /C-oxide- Impregnation method: **19**

3.8 Synthesis of Cobalt promoted Molybdenum sulfide MoS_2/C- Citrate .Impregnation method: **20**

3.9 Sample Characterization **20**

3.10 Activation of the Catalysts **21**

3.11 Activity Measurement **21**

CHAPTER 4 22

RESULTS AND DISCUSSION 22

4.1Elemental Analysis **22**

4.2 Electron Microscopy: **24**

4.3 X- Ray Diffraction: **30**

4.4 Nitrogen Adsorption/ Desorption and BET: **32**

4.5 Catalysts Activity **37**
4.5.1 Catalytic Activity of MoS_2/C-Oxide: 39
4.5.2 Catalytic Activity of MoS_2/C-Cit: 41
4.5.3 Catalytic Activity of (Co)MoS_2/C-Oxide: 43
4.5.4 Catalytic Activity of (Co)MoS_2/C-Cit: 45
4.5.5 Catalytic Activity of (Co)MoS_2/C-Cit -IMP: 47
4.5.6 Catalytic Activity of (Co)MoS_2/C-Oxide -IMP: 49

4.6 Kinetic Treatment **50**

4.7 Model Reaction Fitting **56**

4.8 Catalyst evaluation by desulfurization of model FCC gasoline using microreactor: 60

CHAPTER 5 64

CONCLUSION AND RECOMMENDATIONS 64

5.1 Conclusion 64

5.2 Recommendations: 65

REFERENCES 66

VITAE 70

LIST OF TABLES

Table 2.2 Typical Sulfur Compounds and Corresponding Refinery Streams for Fuels 6
Table 4.1 Elemental analysis of the Synthesized Catalysts 23
Table 4.2 BET analysis of prepared catalysts 33
Table 4.3 overall and individual apparent rate constants for the HDS of DBT at 320°C (10^{-3}/min) 59

LIST OF FIGURES

Figure 2.1 Mechanism of Desulfurization of DBT and 2-Methyl Thiophene 9
Figure 3.1 Five necks flask for PMMA Synthesis 16
Figure 4.1 PMMA Spheres 25
Figure 4.2 Hollow Carbon Sphere 26
Figure 4.3 MoS_2/ C- Oxide 27
Figure 4.4 MoS_2C- Cit 28
Figure 4.5 TEM image of MoS_2/ C- Oxide 29
Figure 4.6 XRD Pattern of Synthesized Catalysts 31
Figure 4.7 Nitrogen Adsorption/Desorption Isotherms of MoS_2/C-Oxide and MoS_2/C-Cit 34
Figure 4.8 Nitrogen Adsorption/Desorption Isotherms of(Co) MoS_2/C-Oxide and (Co)MoS_2/C-Cit 35
Figure 4.9 Nitrogen Adsorption/Desorption Isotherms of(Co) MoS_2/C-Oxide-IMP and (Co)MoS_2/C-Cit-IMP 36
Figure 4.10 Products of HDS of DBT over MoS_2/C oxide 40
Figure 4.11 Products of HDS of DBT over MoS2/C oxide 42
Figure 4.12 Products of HDS of DBT over (Co)MoS_2/C Oxide 44
Figure 4.13 Products of HDS of DBT over (Co)MoS_2/C Oxide 46
Figure 4.14 Products of HDS of DBT over (Co)MoS_2/C-Cit-IMP 48
Figure 4.15 Proposed reaction network for the HDS of DBT 52
Figure 4.16 Products of HDS of DBT over (Co)MoS_2/C-Oxide-IMP 53
Figure 4.17 Product Selectivity vs. conversion of DBT at 320°C for $CoMoS_2$/ C- Oxid-IMP 57
Figure 4.18 Pseudo-first order plot of the HDS of DBT over $CoMoS_2$/ C- Oxide-IMP .. 58
Figure 4.19 Performance of Synthesized catalyst in hydrodesulfurization of 2-MT in Model FCC-Gasoline 62
Figure 4.20 Performance of Synthesized catalyst in hydrogenation of 2,3DM2B in Model FCC-Gasoline 63

LIST OF ABBREVIATIONS

BCH	:	Bicyclohexyl
BET	:	**Brunauer–Emmett–Teller Theory**
BP	:	Biphynel
C_{BCH}	:	Concentration of BCH at a given reaction time
C_{BP}	:	Concentration of BP at a given reaction time
C_{DBT}	:	Concentration of DBT at a given reaction time
DBT	:	Dibenzothiophene
DDS	:	Direct Desulfurization
GC	:	Gas Chromatograph
HCS	:	Hollow Carbon Sphere
HDS	:	Hydrodesulfurization
HYD	:	Hydrogenation
k	:	Reaction rate constant
K	:	Equilibrium constant
MoS_s	:	Molybdenum disulfide

PPM	:	Parts Per Million
R_{DDS}	:	Rate of direct desulfurization
R_{HYD}	:	Rate of hydrogenation
SEM	:	Scanning Electron Microscopy
TEM	:	Transmission Electron Microscopy
THDBT	:	Tetra hydrogenated dibenzothiophene
XRD	:	X-ray diffraction

ABSTRACT

Full Name : [Abdullah Faisal Al-Ahmadi]

Thesis Title : [SYNTHESIS, CHARACTERIZATION AND EVALUATION OF (Co)MoS2 HDS SUPPORTED ON HOLLOW CARBON SPHERE FOR DESULFURIZATION OF THIOPHENE]

Major Field : [Chemistry]

Date of Degree : [May 2013]

Hollow carbon spheres containing varying amounts of molybdenum and cobalt with up to 18% molybdenum were synthesized. Materials were prepared using poly-Methylmetacrylate templates to support the growth of resorcinol formaldehyde resin. The resulting solid was calcined under nitrogen to produce hollow carbon spheres.

Supported cobalt promoted Molybdenum sulfides were synthesized using co-condensation and impregnation of molybdenum and cobalt on the surface of hollow carbon spheres. Scanning electron microscopy and transmission electron microscopy showed the dispersion and of molybdenum on the surface of support and the stability of spherical structure of hollow carbon spheres.

X-ray diffraction revealed the presence of molybdenum sulfide phase and cobalt sulfide phase. All catalysts exhibited high activity in overall hydrodesulfurization (HDS) reaction of dibenzothiophene (DBT). Kinetic analysis of the reaction data showed that the contribution of direct desulfurization (DDS) route predominates over hydrogenation (HYD) route in HDS of DBT for all catalysts.

ملخص الرسالة

الاسم الكامل: عبدالله فيصل الأحمدي

عنوان الرسالة: تحضير و توصيف و دراسة الفاعلية تجاه الإزالة الهيدروجينية للكبريت لحفازات كبريتيد الملوبدينوم المنشطة بالكوبالت و المدعومة على كريات الكربون المفرغة

التخصص: الكيمياء

تاريخ الدرجة العلمية: مايو-2013

تم في هذه الرسالة تحضير مركبات الكربون الكروية المفرغة و التي تحتوي على كميات مختلفة من الملوبدينوم و الكوبالت بنسب وزنية مختلفة تصل إلى 18%. تم التحضير بإستخدام البولي ميثيل ميثاكريلات كأساس لنمو مزيج الريسورسانول و الفورمالدهيد. تم حرق المزيج السابق في وجود غطاء من النيتروجين لإنتاج كريات الكربون المفرغة.

تم اضافة المولبدينوم و الكوبالت على سطح كريات الكربون المفرغة بإستخدام طريقة التكثيف المشترك لمحاليل الملوبدينوم و الكوبالت و كذلك طريقة الترسيب المباشر على سطح كريات الكربون المفرغة. تم توصيف المواد المحضرة بإستخدام المجهر الألكتروني الماسح و النفاذ و التي اظهرت توزيع المولبدينوم على السطح الداعم و كذلك ثبات الشكل الكروي للسطح الداعم. تم استخدام الحيود السيني الذي اثبت وجود المولبدينوم النشط و كذلك مركبات كبريتيد الكوبالت. جميع المواد الحفازة اظهرت نشاط عالي في الإزالة الهيدروجينية للكبريت عند استخدام نموذج من مركب ثنائي بنزين الكبريت. تحليل الحركية الكميائية اظهر ان ميكانيكية التفاعل يغلب عليه مسار الإزالة المباشرة للكبريت بدلا من مسار الهدرجة في كل الحفازات المستخدمة في هذه الدراسة.

CHAPTER 1

INTRODUCTION

Crude oil is a complex mixture of hydrocarbons with different C/H ratio and molecular structures. The main classes of hydrocarbon molecules are paraffins, olefins, cyclic paraffins, aromatics, asphaltenes, and other poly-unsaturated molecules. In addition to hydrocarbons, crude oils also contain some other compounds containing atoms other than carbon and hydrogen (heteroatoms). Those compounds may contain sulfur, nitrogen, oxygen, and heavy metals such as iron, nickel, and vanadium. Crude oil is usually classified based on specific gravity as extra light, light, medium, heavy, and extra heavy. An empirical set of units for the crude gravity, defined by the American Petroleum Institute (API), is currently used in oil industry. Light crude oil has lower specific gravity and larger API gravity, and the opposite for heavy crude oil. Also crude oil is classified based on the sulfur content and composition. *Sour* crude oil indicates high sulfur content and sweet crude oil indicates low sulfur content. Meanwhile, "paraffinic" crude oil is mainly composed of paraffins, "naphthenic" for high content of cyclic paraffins, and "aromatic" for high content of aromatic compounds [1-3].

Modern oil refinery is a complex and integrated plant. Its task is to produce more valuable products from the supplied crude oil. The main products are liquefied petroleum gas, transportation fuels, wax, lubricants and bitumen[1].

Compliance with the environmental regulations regarding the quality of transportation fuels and emission is a major issue. The main objective of environmental regulations proposed by environmental protection agency (EPA) and European Parliament is to reduce the sulfur content of fuel to less than 10 ppm by 2009 and further to nearly zero in the future. Since gasoline, diesel and non-transportation fuels represent 75-80% of overall refinery products, these regulations will have significant impact on refinery operation. Another major issue is the declining quality of crude oil supplies. Heavy and sour crude became the dominant type in the crude oil market. This added more pressure on refineries to meet the products specifications based on poor feedstock[1-3].

Hydrotreating and hydrodesulfurization (HDS) of middle distillate streams are required to achieve the desired specifications. Among several approaches that have been made, the development of more active and stable catalyst is favored. The typical catalyst used for hydrodesulfurization in most refineries is based on transition metal sulfides supported on alumina and it is known as conventional HDS. However conventional HDS ability to remove sulfur from the least reactive thiophenes is limited. This issue derived the refiners to implement more advanced hydrodesulufrization process and/or implement more treatment processes[3-4].

A large number of researches in recent years focused on finding more effective catalysts for desulfurization of least reactive sterically hindered alkylthiophene, dibenzothiophene and alkylated dibenzothiophene. Interesting results regarding catalytic activity of new phases such as carbides, phosphides and nitrides were observed. However, sulfide based formulations consists of molybdenum sulfide with or without promoting metals, such as cobalt, nickel, supported on alumina appear to be the most promising catalyst[5-6].

Gasoline is produced by blending the straight run naphtha from the distillation units and naphtha from fluid catalytic cracking unit (FCC). Most sulfur come with FCC product stream. So the treatment of FCC gasoline is critical. Another issue to considered regarding FCC gasoline is the fact that olefins is the major contributor to the octane number of FCC gasoline. However, desulfurization process leads also to reduction in olefins content and lead to loss of octane number. For this reason, an effective catalyst for desulfurization of FCC gasoline should exhibit a minimum hydrogenation of olefins[7].

1.1 Research Objectives:

The following are the objectives of the thesis:

1- To synthesize a supported (Co)MoS_2 catalyst on hollow carbon spheres.
2- To characterize the catalyst in order to ascertain the chemical and morphological properties.
3- To evaluate the activity of the catalyst on hydrodesulfurization (HDS) of Dibenzothiophen(DBT) and 2-Methyl Thiophene

CHAPTER 2

LITERATURE REVIEW

2.1 Review of Hydrodesulfurization Catalysis Technologies:

In order to meet the growing demand for ultra-low sulfur fuel and comply with strict environmental regulations, a number of new concepts and technologies have been developed in the last 20 years in addition to the choice of revamping the conventional hydrotreating units. It has reported that most of hydro treating units were installed to meet the 1993 low sulfur content (500 ppm) can be revamped for ultra-low sulfur fuel (10 ppm) production with acceptable increase in operational cost. Several options such as variation of process conditions and finding more soft oil feed have been explored. Also the use of highly active new catalyst was given a lot of importance[7].The use of highly active catalyst can improve the performance of existing hydrodesulfurization units.

New catalysts have been developed by major companies. Cosmo oil developed C-606A with 3 times higher HDS activity compared to the conventional $CoMo/Al_2O_3$ [8].

Akzo Nobel came up with STARS catalyst series, which show almost double HDS rate. In recent time, Akzo Nobel offered a new catalyst known as NEBula. It is made of unsupported bulk sulfides of group VIII and VI metals and provided increased HDS reactivity by four folds.

Topøse developed a series of catalyst , TK-573, TK-574, TK911 and TK-915, which not only developed the desulfurization activity, but also talked density and aromatics reduction Topøse also developed a new catalyst preparation technology BRIM, giving highly active hydrogenation catalysts. BRIM not only optimize the hydrogenation site, but also increase type II activity sites for direct desulfurization. The first two commercial catalysts based on the BRIM technology were Topøse TK-558 BRIM (CoMo) and TK-559 BRIM (NiMo) for FCC pretreatment service. This was followed by a series of new high performance catalysts TK-575 BRIM (NiMo), TK-576 BRIM (CoMo), and TK-605 BRIM catalyst for ultra-low sulfur diesel production and for hydrocracker feed pretreatment[9]. Research in developing high performance catalysts will continue to play a key role on achieving the clean fuel requirements.

2.2 Sulfur Impurities in FCC Gasoline:

The main sulfur components of FCC gasoline are thiols, sulfides, thiophene and alkylthiophenes, tetrahydrothiophene, thiophenols and benzothiophene Alkylthiophenes which are typically in the boiling range of gasoline include three and four carbon atoms-substituted thiophenes (C3- and C4-thiophenes). Recent data reported by Xia and coworkers confirm that thiophene sulfur represents a large fraction of the total sulfur content in FCC gasoline (60 wt.% and over). By using gas chromatography they detected more than 20 different kinds of thiophenes among which a certain number (di- and trimethyl-, ethyl-, ethylmethyl-, di- and triethyl-, iso-propyl-, tertiobutyl-) could be identified by GC/MS analysis [3].

Table 2.1: Typical Sulfur Compounds and Corresponding Refinery Streams for Fuels

Sulfur compounds	Refinery streams	Corresponding fuels
Mercaptanes, RSH; sulfides, R2S; disulfides, RSSR; thiophene (T) and its alkylated derivatives, benzothiophene	SR-naphtha; FCC naphtha; coker naphtha	Gasoline (BP range: 25–225 °C)
Mercaptanes, RSH; benzothiophene (BT), alkylated benzothiophenes	Kerosene; heavy naphtha; middle distillate	Jet fuel (BP range: 130–300 °C)
Alkylated benzothiophenes; dibenzothiophene (DBT); alkylated dibenzothiophenes	Middle distillate; FCC LCO; coker gas oil	Diesel fuel (BP range: 160–380 °C)
Greater than or equal to three-ring polycyclic sulfur compounds, including DBT, benzonaphthothiophene (BNT), phenanthro[4,5-b,c,d]thiophene (PT)	Heavy gas oils; vacuum gas oil; distillation resides	Fuel oils (non-road fuel and heavy oils)

2.3 HDS Reactivity of Sulfur Compounds:

It has been established by several research studies that the relative reactivates of thiopene based sulfur compounds are significantly different [10-12]. This could be attributed to the conjugative interaction between the lone pair of electrons on sulfur atom and the π- system of aromatic ring. The reactivity of sulfur compounds in HDS follows this order (from most to least reactive): thiophene > alkylated thiophene > BT > alkylated BT > DBT and alkylated DBT without substituents at the 4 and 6 positions > alkylated DBT with one substituent at either the 4 or 6 position > alkylated DBT with alkyl substituents at the 4 and 6 positions. This trend has been attributed to the steric hindrance of the substituent alkyl group which prevents interaction between sulfur atom and the catalytic active site[12]. Also the electronic inductive effects between the alkyl groups on the ring and sulfur atom enrich the electron density on the sulfur.

2.4 Mechanism of HDS reactions:

In order to design an effective catalyst for the production of ultra low sulfur fuels, the various kinetic pathways of hydeordesulfurization (HDS) reactions must be understood.

For a typical thiophene based sulfur compounds, it has been established that HDS reaction proceeds through two parallel and consecutive routes: direct desulfurization (DDS) and desulfurization through hydrogenation (HYD).

For example, hydrodesulfurization of dibenzotiophene through (DDS) will yield a bi-phenyl type compound (BP). Or it will undergo through (HYD) to produce tetrahydrodibenzothiophene (THDBT). Depending on the conditions of reaction, THDBT can be further hydrogenated to produce cyclohexanebenzene type compound (CHB)[11,13,14]. CHB can be further hydrogenated to produce bi-cyclohexane. As shown in figure 2.1

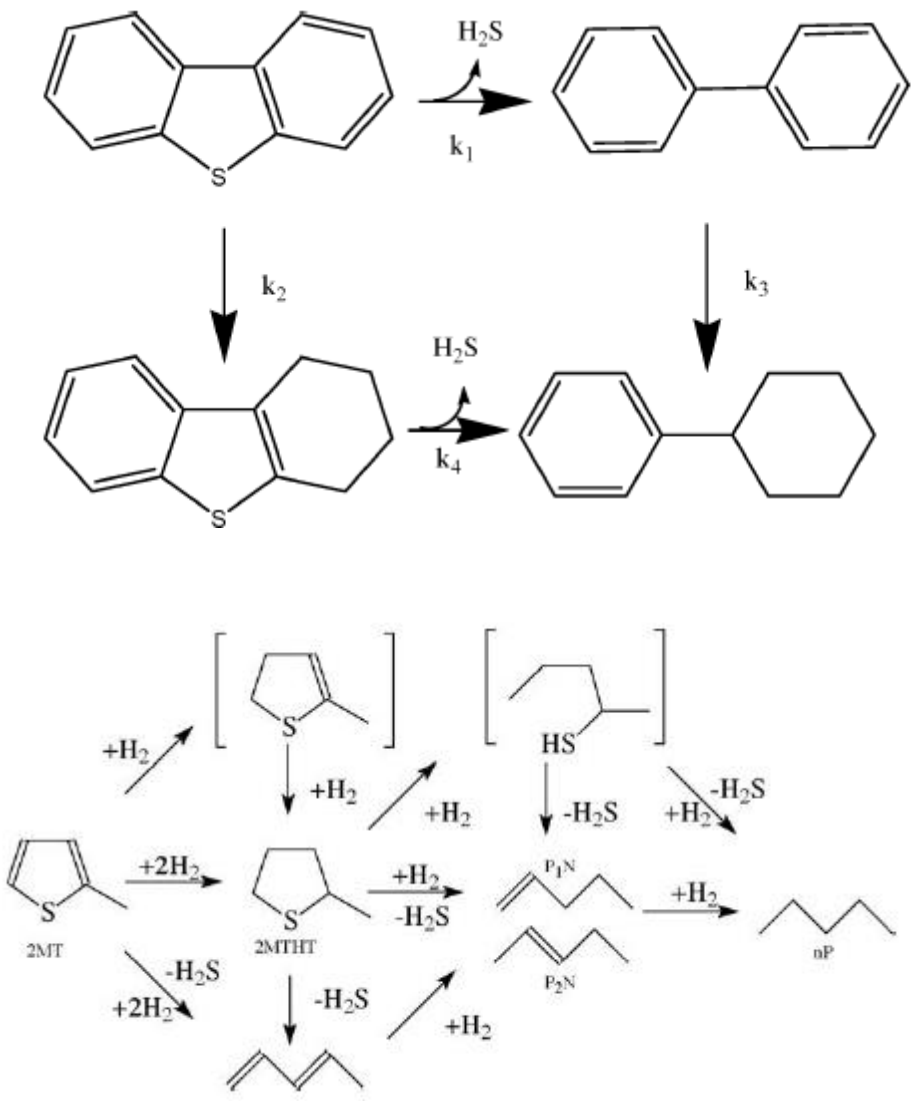

Figure 2.1 Mechanism of Desulfurization of DBT and 2-Methyl Thiophene

2.5 Supported Catalysts:

The active phase in a HDS catalyst is usually deposited on the surface of another martial called support. The support material usually provides a high surface area to maximize the active phase dispersion and to provide mechanical strength to the catalyst. Common supports used are Al_2O_3 , ZrO_2 ,TiO_2, SiO_2, Zeolites and carbon material. Alumina is the most widely used support material in industry because of its favorable chemical, physical, and mechanical properties on one hand and its availability and cost on the other hand[15].

For several decades, CoMo and NiMo/alumina have been used in industrial refining plants as HDS catalyst. Since the proposal of Topsøe and coworkers, there has been a growing interest in CoMoS and NiMoS phases, in which Co or Ni decorate the edge sites in CoMo and NiMo sulfide catalysts and many spectroscopic aspects have been interpreted based on this model. Topsøe differentiated between CoMoS phases, Type I and Type II, depending on their HDS activity. CoMoS Type II, which formed by high temperature sulfidation 600-1000 C^o, was about twice as active as Type I, which formed by sulfidation at 400 C^o[16]

It has also been reported by several authors that variation of the support influences the electronic and catalytic properties of supported CoMo and NiMo sulfide catalysts. This is because the changes in support lead to variation a in active phase support interaction that influences the dispersion and morphology of active-phase components. The strength of interaction between the active metals and support affects the reducibility and sulfidabilty of active phase. For example, studies have shown strong interaction between molybdate and the alumina support lead to formation of Mo-O-Al linkage after sulfidation. This mean a further increase in HDS activity of supported sulfide catalysts can be achieved by changing the support[17-20].

The development of new supports has received great attention because of the need to develop better HDS catalysts .TiO_2, ZrO_2, SiO2, Zeolites, and carbon materials of high surface area and good properties have been developed and tested. TiO_2 and ZrO_2 supported MoS_2 catalyst shown three to five times respectively higher hydrodesulfurization and hydrogenation activity than alumina supported one with an equivalent Mo loading per nm^2[21].

2.6 Carbon Support:

2.6.1 Poly Methyl Methacrylate Latex Templates:

Poly(methyl methacrylate) used as sacrificial template to synthesis the carbon hollow spheres. poly(methyl methacrylate) (PMMA) latex spheres were synthesized according to published methods[22-23].

2.6.2Tailoring the Diameter of the Product:

Four factors influence the size of the latex spheres produced in this synthesis: the concentration of the monomer, the concentration of the initiator, the ionic strength of the reaction mixture, and the reaction temperature. Increasing the monomer concentration or the ionic strength increases the diameter of the particles produced; increasing the concentration of the initiator or the reaction temperature decreases the diameter.

The ionic strength is increased by adding a monovalent, water-soluble salt, most commonly sodium chloride. The maximum ionic strength is about $2x10^{-2}$. Increasing the ionic strength further causes the latex to coagulate during the reaction. For potassium persulfate-initiated polymerization, the effect of initiator concentration on particle size is effectively canceled out by a concurrent increase in ionic strength of the reaction medium.

Goodwin et al. parameterized the relationship between size and reaction variables for the formation of PS latex spheres A least-squares fit to the data given by Tanrisever et al. allowed the parameters for PMMA spheres to be determined as well. The general equation and parameters for PS and PMMA spheres predicts the final size of the spheres within 10% error for PMMA. Based on experiment, the equation is valid for PMMA sphere diameters between 80 nm and 450 nm. The range of temperature at which the reaction has been carried out successfully (i.e., reactions that have produced uniform sphere diameters) is 55-90 °C. Attempts to produce spheres outside of these ranges resulted in non-uniform diameters or coagulation of the mixture[22-24].

2.6.3 Carbon Spheres:

In the past decades, carbon materials experienced great development because of their potential applications in energy storage and conversion, adsorption, catalysis, and other applications. It has been possible to synthesize carbon materials with defined nanostructure and morphology, tunable surface area, and pore volume. For convenience, these materials are grouped into four categories: 0D quantum dots and spheres; 1D fiber, tubes, and wires; 2D films and membranes; and 3D structure of Diamond. Carbon spheres are usually prepared by carbonization of polymer precursors. In this case, polymer precursors are required to be thermally stable and are able to form carbon residue after a high-temperature pyrolysis. Phenolic resins, derived from the polymerization of phenols (phenol, resorcinol,) with aldehyde (e.g., formaldehyde), are attractive because of their excellent performance characteristics such as high-temperature resistance, thermal abrasiveness, and high yield of carbon conversion [25].

Carbon spheres can be synthesized by different methods such as hydrothermal, self-assembly and templating method. Templating is considered to be the most straightforward way to create hollow sphere structure. Soft templating , using surfactant or polymer precourceor, and hard templating, using different solid core such as silica or iron, were used to synthesize hollow carbon spheres[25-26].

CHAPTER 3

Experimental

3.1 Synthesis of Polymethylmethacrylate (PMMA) Dispersion:

3.1.1 Apparatus:

A schematic of the apparatus used to make the latex is shown in Figure 3.1. It consisted of a five-neck, 2-L round-bottom flask which sat in mantle heating well. A 44-cm long, 1-cm wide, polished glass shaft supported by a lubricant-free Teflon Trubore bearing with a glass thread adapter is fed through the center neck of the flask. Inside the reaction vessel, a 75-mm long, crescent-shaped PTFE blade was attached to the shaft. A variable-speed motor was coupled to the glass shaft through fitted rubber vacuum tubing and rotated the blade assembly at rates up to 800 rpm. During a typical polymer synthesis, the mixing blade was spun at 300-500 rpm. The rotational frequency was calibrated with a strobe light.

Nitrogen gas was bubbled through a Pasteur pipette. The pipette was held in place by a rubber, one-hole stopper placed in one of the necks of the reaction flask. The tip of the pipette was inserted below the surface of the liquid to displace dissolved oxygen in the reaction mixture and to blanket the reaction in inert gas. A clean, new pipette was used for each synthesis.

3.1.2 Synthesis:

Mono dispersed poly-methylmethacrylate spheres were synthesized via emulsifier-free emulsion polymerization of methyl-methacrylate in water as solvent and under nitrogen

blanket to establish inert atmosphere. Four batches of PMMA prepared by adding a measured volumes of MMA and double distilled water is added to prepare a 2000ml solution. Initially, the solution is stirred and heated to 70C^{o} under nitrogen atmosphere for one hour to remove the inhibitor from commercial MMA. Then 0.5 g of initiator, (2.2-Azobis(2-methyl) propionamidine) dihydrochloriden97%, was added to MMA solution. The solution kept stirring at 70C^{o} for three hours until the completion of polymerization reaction.

Sample was taken from the polymerization product and dried to calculate the percentage of solid in polymer solution. The resulted solid concentration were (4.367, 6.48, 8.96, 18.6 %) respectively.

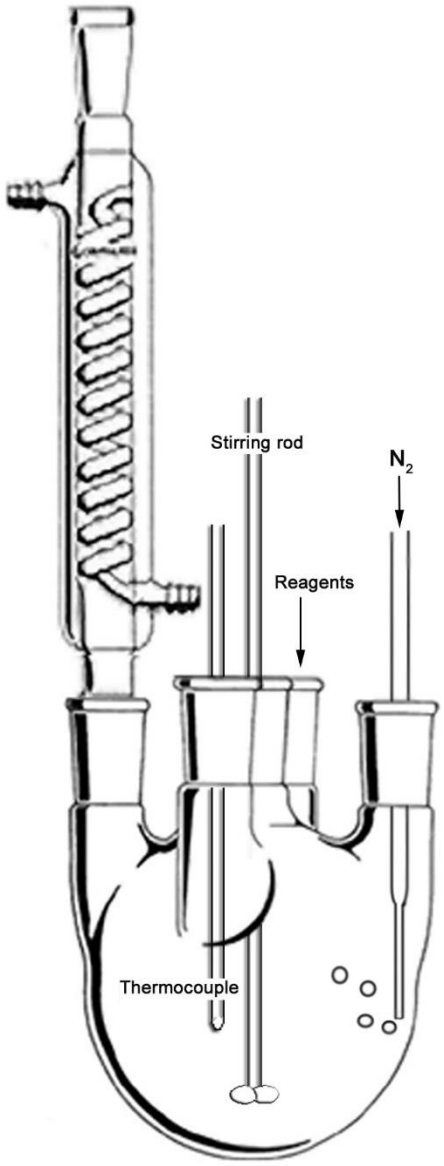

Figure 3.1 Five necks flask for PMMA Synthesis

3.2 Synthesis of Carbon Latex Using Resorcinol- Formaldehyde Resin:

12.9 g of para-formaldehyde was dissolved in 100 ml water. Subsequently, 193 g of PMMA latex dispersion (18.6%) was added. The mixture was stirred at 50C^{o} for 24 hours. The solution was then allowed to cool to room temperature and an extra 100 ml of distilled water was added. Then 0.52g of diaminohexane was added to the previous solution and stirred at room temperature for 15 min to reach pH 9.4. 22.5 g of resorcinol dissolved in 40 ml distilled water was added to the previous solution and stirred for 15 min at room temperature. The dispersion sealed and stirred at 85 C^{o} for 18 hours. The dispersion was then allowed to cool to room temperature, filtered and dried at 100 C^{o} for 24 hours. The resulted solid was calcined under nitrogen at 330°C for 2 h using a ramp step of 5°C per min, then increased to 500 C^{o} for 4hou h using a ramp step of 5°C per min.

3.3 Synthesis of Molybdenum Sulfide MoS_2/C-Oxide:

7.197 g of molybdenum oxide (MoO_3) was dissolved in 15 ml 37% HCl and heated overnight at 85C^{o} in a sealed flask. The resulted solution allowed cooling to room temperature. 25 ml of water and 10 ml of ethanol were added to the metal solution. 3.5 g of PMMA- RF solid was socked with the above solution. Then filtered using vacuum filtration and dried at 85C^{o} for 24 hours. The dried sample then calcined under nitrogen at 330°C for 2 h using a ramp step of 2°C per min, then increased to 500 C^{o} for 4hour using a ramp step of 2°C per min.Then the sample was sulfided under 10%H_2S balanced with hydrogen at 375C^{o} for 2 hours using a ramp step of 5 C^{o}/ min. The molybdenum content was 18.87wt% using EDS.

3.4 Synthesis of Molybdenum sulfide MoS_2 /C-Citrate:

8.827 g of $(NH_4)Mo_7O_{24}.6H_2O$) and 10.52 g of citric acid were dissolved in 50 ml solution of 40 ml water and 10 ml ethanol. 3.5 g of PMMA- RF solid was soaked in the above solution, filtered using vacuum filtration and dried at 85C^o for 24 hours. The dried sample was calcined under nitrogen at 330°C for 2 h using a ramp rate of 2°C per min, then increased to 500 C^o for 4hour using a ramp step of 2°C per min. The sample was then sulfided under 10%H_2S balanced with hydrogen at 375C^o for 2 hours using a ramp step of 5 C^o/ min. The molybdenum content was 12.05 wt% measured by EDS**.**

3.5 Synthesis of Cobalt promoted Molybdenum sulfide $CoMoS_2$ /C-Citrate:

6.7904 g of $(NH_4Mo_7O_{24}.6H_2O)$, 3.358g of $Co(NO_3)_2.6\ H_2O$, and 10.52 g of citric acid were dissolved in 50 ml solution of 40 ml water and 10 ml ethanol. 3.5 g of PMMA- RF solid was socked with the above solution. Then filtered using vacuum filtration and dried at 85C^o for 24 hours. The dried sample then calcined under nitrogen at 330°C for 2 h using a ramp step of 2°C per min, and then increased to 500 C^o for 4hour using a ramp step of 2°C per min. Then the sample was sulfided under 10%H_2S balanced with hydrogen at 375C^o for 2 hours using a ramp step of 5 C^o/ min. The molybdenum and cobalt contents were 4.78 wt% and 0.84 wt% respectively using EDS

3.6 Synthesis of Cobalt promoted Molybdenum sulfide $CoMoS_2$ /C-Oxide:

5.5362 g of molybdenum oxide (MoO_3) was dissolved in 20 ml 37% HCl and heated overnight at 85C^o in a sealed flask. The resulted solution was allowed to cool to room temperature. Adding 3.358 g of $Co(NO_3)_2.6\ H_2O$, to above molybdenum solution and heated with stirring for 24 hours at 85 C^o in a sealed flask . Once, allowed to cool to room temperature, 20 ml of water and 10 ml of ethanol were added to the solution, followed by soaking 3.5 g of PMMA- RF in the above solution. Then filtered using vacuum filtration and dried at 85C^o for 24 hours. The dried sample then calcined under nitrogen at 330°C for 2 h using a ramp rate of 2°C per min, and at 500 C^o for 4hour using a ramp rate of 2°C per min. The sample was then sulfided under 10%H_2S balanced with hydrogen at 375C^o for 2 hours using a ramp rate of 5 C^o/ min. The molybdenum and cobalt contents were measured to be14.32 wt% and 1.65wt% respectively using EDS.

3.7 Synthesis of Cobalt promoted Molybdenum sulfide $CoMoS_2$ /C-oxide-Impregnation method:

In order to achieve the targeted mole ratio of 1 mol Mo: 0.3 mol Cobalt, 1.202g of Co $(NO_3)_2.6\ H_2O$ was dissolved in a mixture of 5 ml water and 7 ml methanol. 7 g of MoS_2/C-oxide base was soaked in the cobalt solution, mixed well and dried at 100C^o for 24 hours. Then the dried sample was sulfided under 10%H_2S balanced with hydrogen at 375C^o for 2 hours using a heating rate of 5 C^o/ min.

3.8 Synthesis of Cobalt promoted Molybdenum sulfide MoS_2/C- Citrate .Impregnation method:

In order to achieve the targeted mole ratio is 1 mol Mo: 0.3 mol Cobalt, 0.5483g of Co $(NO_3)_2$.6 H_2O was dissolved in a mixture of 5 ml water and 7 ml methanol. 5 g of MoS_2/C –Citrate was soaked in the cobalt solution, mixed well and dried at 100C^o for 24 hours. Then the dried sample was sulfided under 10%H_2S balanced with hydrogen at 375C^o for 2 hours using a heating rate of 5 C^o/ min.

3.9 Sample Characterization

Field Emission Scanning Electron Microscopy: The morphology of samples was investigated using scanning electron microscopy. energy dispersive spectroscopy(EDS) was used to determine the composition of samples for carbon, sulfur, cobalt and molybdenum content.

N_2 Adsorption/Desorption Isotherm and BET : Nitrogen adsorption/desorption isotherms were acquired using Quantachrom Autosorb-1c . Specific surface area was calculated using BET method and pore size distributions were calculated by BJH method and using the desorption branch of the isotherm.

XRD: The x-ray powder diffraction patterns (XRD) were collected on a diffractometer using the Cu Kα line for wide angle in the 2θ range. The XRD data were recorded in the 2θ range from 5 to 80 with a step size of 0.02 with $n\lambda = 2dSin\theta$.

3.10 Activation of the Catalysts

Before the catalytic activity tests, the catalysts were sulfided ex situ in a tubular furnace at 375°C for 2 hours in a stream of 10% H_2S in a balanced H_2. The presulfiding step is necessary to convert the catalyst from oxide form to sulfide form, which is the active phase of the conventional reaction system. The sulfided catalyst was transferred quickly into the batch reactor containing the feed.

3.11 Activity Measurement

Activity measurement was done by carrying out reactions in a 250ml autoclave stirred batch reactor 320C^o. In a typical reaction, 120ml of the feed (about 4000 ppm DBT in decane) was charged into the reactor with 0.5g of the sulfided catalyst. The system was pressurized with nitrogen in order to detect any leak and it was later purged three (3) times with hydrogen. Subsequently, the hydrogen pressure was adjusted to 4MPa and the stirring rate was 500rpm. The reaction system was heated to the desired temperature and allowed to proceed for 3hours. During the reaction, liquid samples of 3-5ml were withdrawn at 15 minutes intervals for 2 hours, then every30 minute in the third hour. Liquid samples were analyzed with Agilent gas chromatograph fitted with capillary HB1 column and fitted with both FID and SCD detectors. These results were used in the kinetic study.

Also the activity measurement was done by carrying out reactions in microreactor with a continuous flow of FCC model Gasoline. The FCC model Gasoline was formulated as follow: (3% 2-Methyl Thiophene, 20% 2,3 di methyl but2-ene, 40% o-xylene 47% n-heptane.

CHAPTER 4

Results and Discussion

4.1Elemental Analysis

The samples were analyzed to determine the content of molybdenum, cobalt, sulfur, carbon and oxygen. The higher loading of molybdenum is desired in order have a maximum possibility of MoS_2 active phase. Catalysts synthesized through oxide route exhibited a higher metals loading than citrate route catalysts. These results are unexpected since citrate complex tends to improve the wettability of metals and carbon surface[31]. But from the SEM images, the citrate catalysts exhibited excessive nicking, which indicate that citric acid worked also as carbon precursor and metals in citrate complex are buried under the carbon layer formed by citrate complex. The elemental analysis results using Energy Dispersal Spectroscopy (EDS) are listed in table 4.1.

Table 4.1 Elemental analysis of the Synthesized Catalysts

Catalyst Name	C wt %	O wt%	S wt%	Mo wt%	Co wt%
MoS2/C- oxide	60	13.96	7.70	18.34	0
MoS2/C- Cit	66.49	10.58	10.28	12.66	0
CoMoS2/C- oxide	56.89	9.93	10.98	17.51	4.68
CoMoS2/C- Cit	68.44	8.84	9.14	11.31	2.28
CoMoS2/C- oxide-IMP	57.41	12.09	10.51	18.14	0.68
CoMoS2/C- Cit-IMP	58.32	9.64	10.01	11.85	2.81

4.2 Electron Microscopy:

The purpose of pursing scanning Electron Microscopy (SEM) and transmission electron microscopy (TEM) is to examine the morphology of the material. SEM analysis is important to determine if there is a nicking between the carbon sphere or not. Also to find the extent of deformation of the hollow carbon spheres. TEM used to observe the dispersion and shape of active metals on the surface of carbon sphere.

The pure hollow carbon sphere showed a high degree of dispersion and undamaged spherical structure and so on in case of MoS_2/ C- Oxide, See figure 4.3. However, MoS_2C-Cit shows a high degree of nicking, see figure 4.4. This is evidence that citric acid is absorbed between RF-PMMA sphere and act as additional source of carbon that lead to excessive nicking.

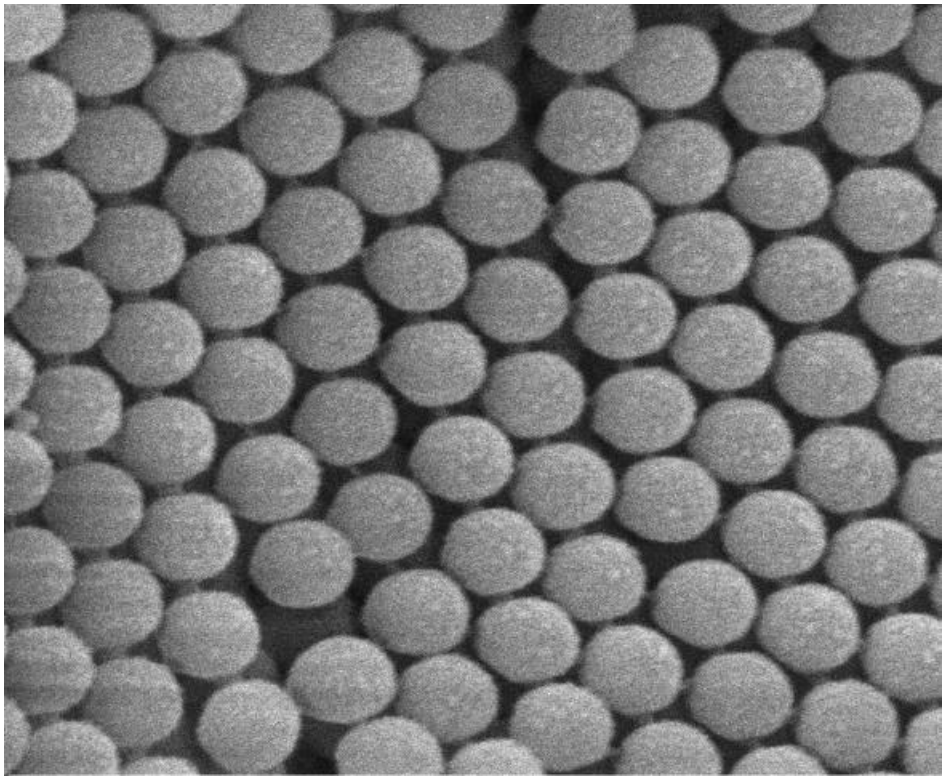

Figure 4.1 PMMA Spheres

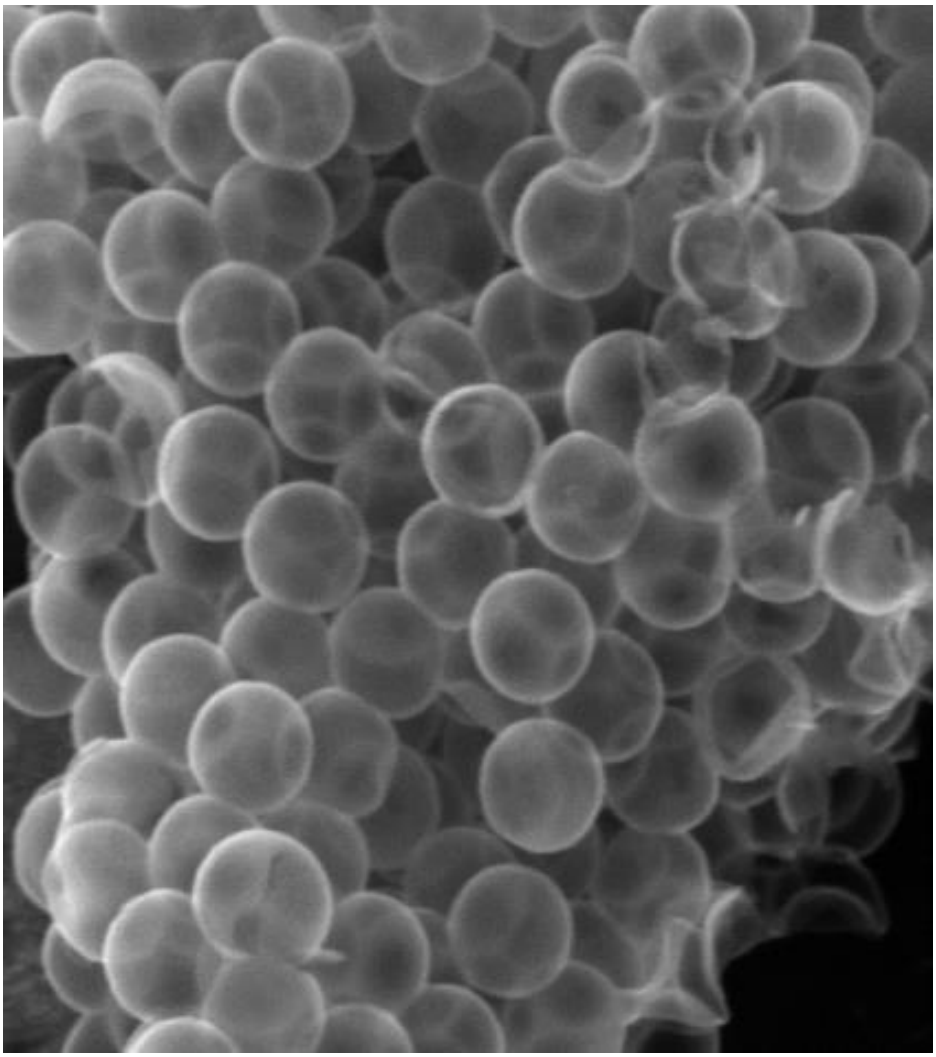

Figure 4.2 Hollow Carbon Sphere

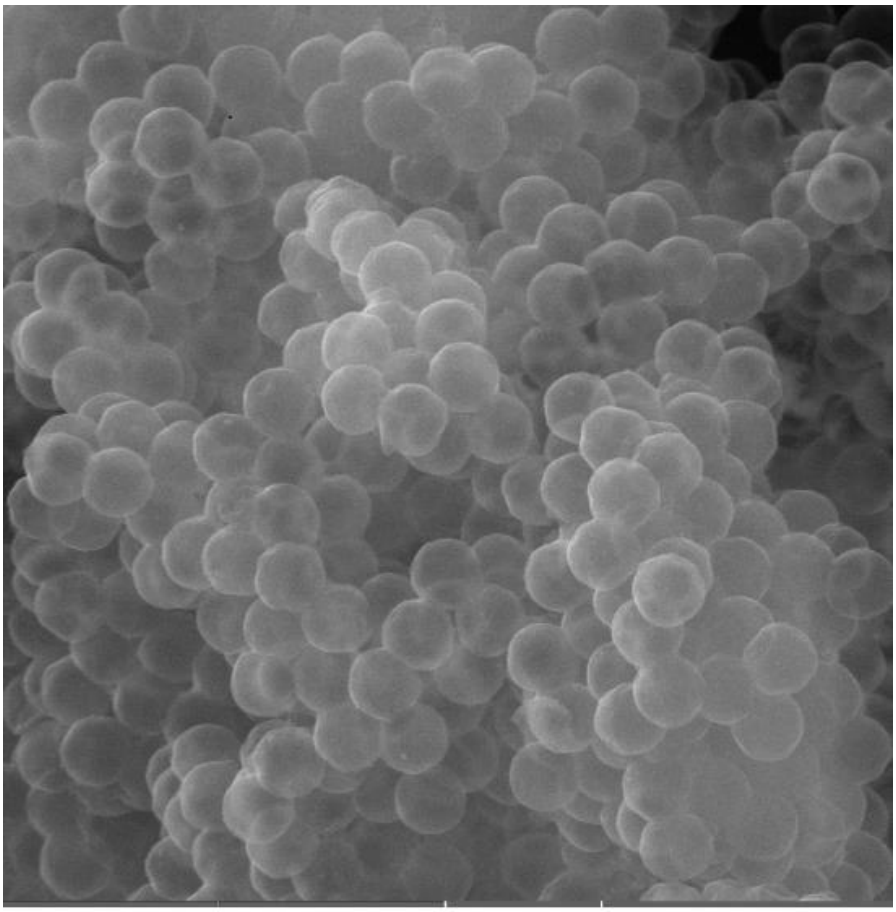

Figure 4.3 MoS_2/ C- Oxide

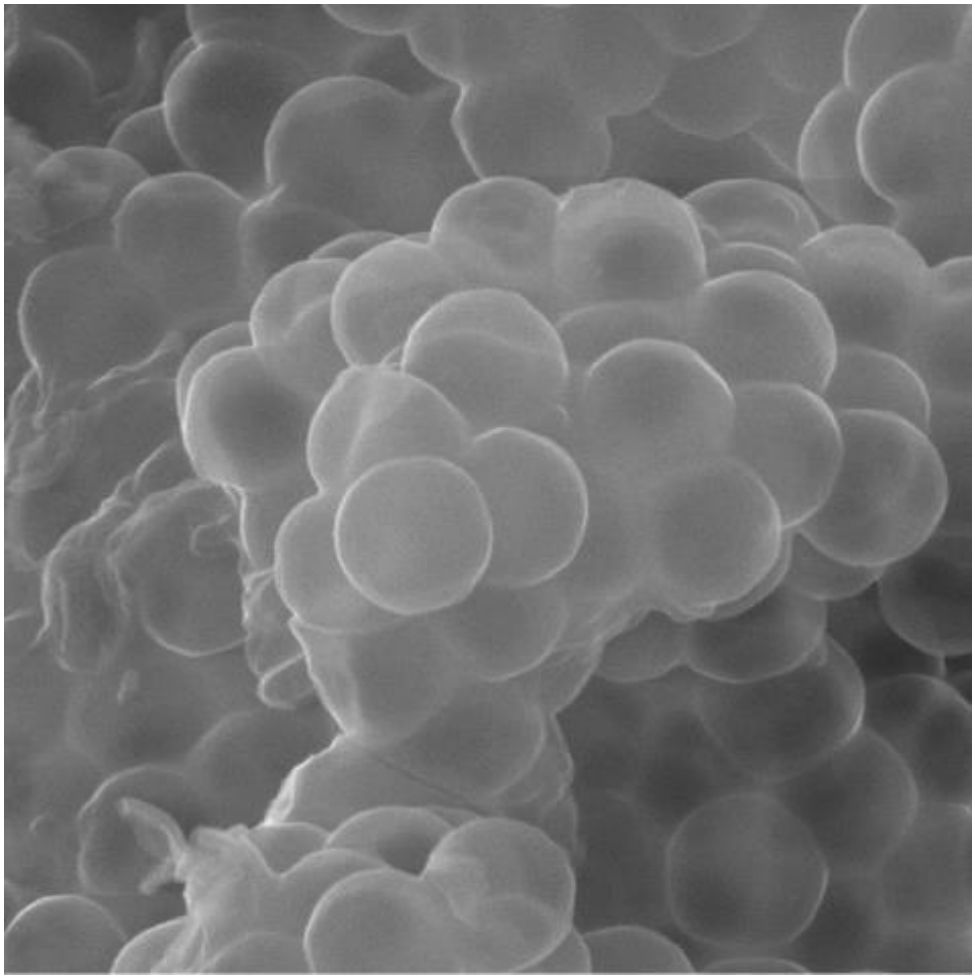

Figure 4.4 MoS_2C- Cit

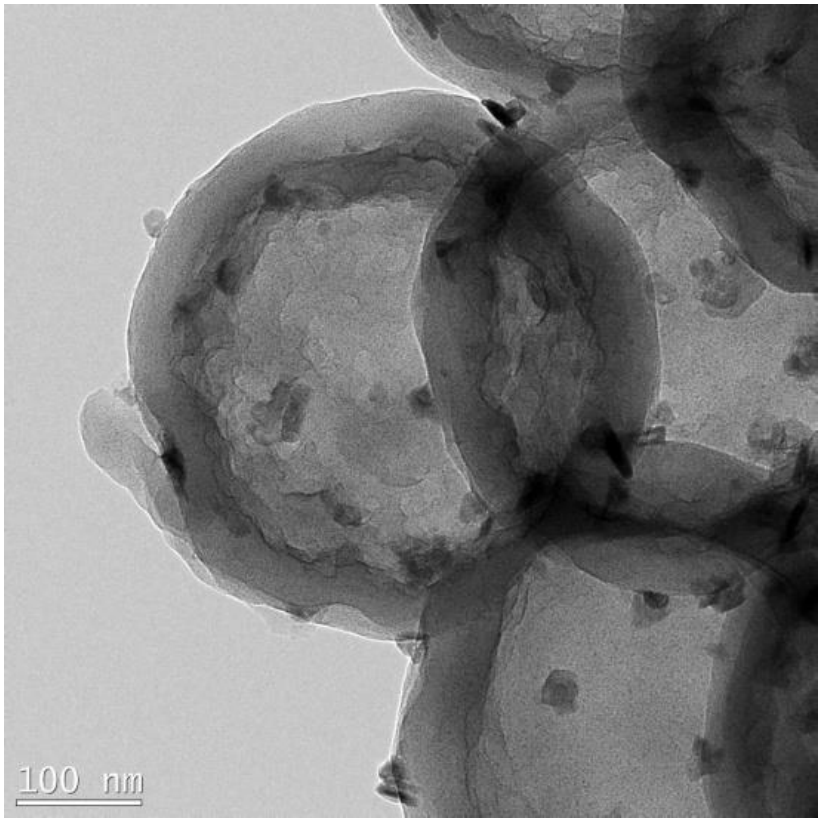

Figure 4.5 TEM image of MoS_2/ C- Oxide

4.3 X- Ray Diffraction:

In the wide angle region where Mo sulfide peaks are expected, intense peak near 14 (2θ) indicate the 002 plane, which is the active phase in hydrodesulphurization.

At 33, 40 and 56 there are peaks for 100, 103, and 110 plans that indicate stacking of MoS_2 Layers. In promoted catalysts, there are additional peaks for Cobalt sulfide phases Co_9S_8 . The peaks for Co_9S_8 indicate the phase separation of cobalt hence not promoted the molybdenum sulfide phase. Catalysts synthesized through citrate route show broad and larger peaks of molybdenum sulfide, which indicates larger crystal size and stacking. Also the peaks of Co_9S_8 are less intense in citrate based catalysts. This indicates less phase separation comparing with catalysts synthesized through oxide route [31]

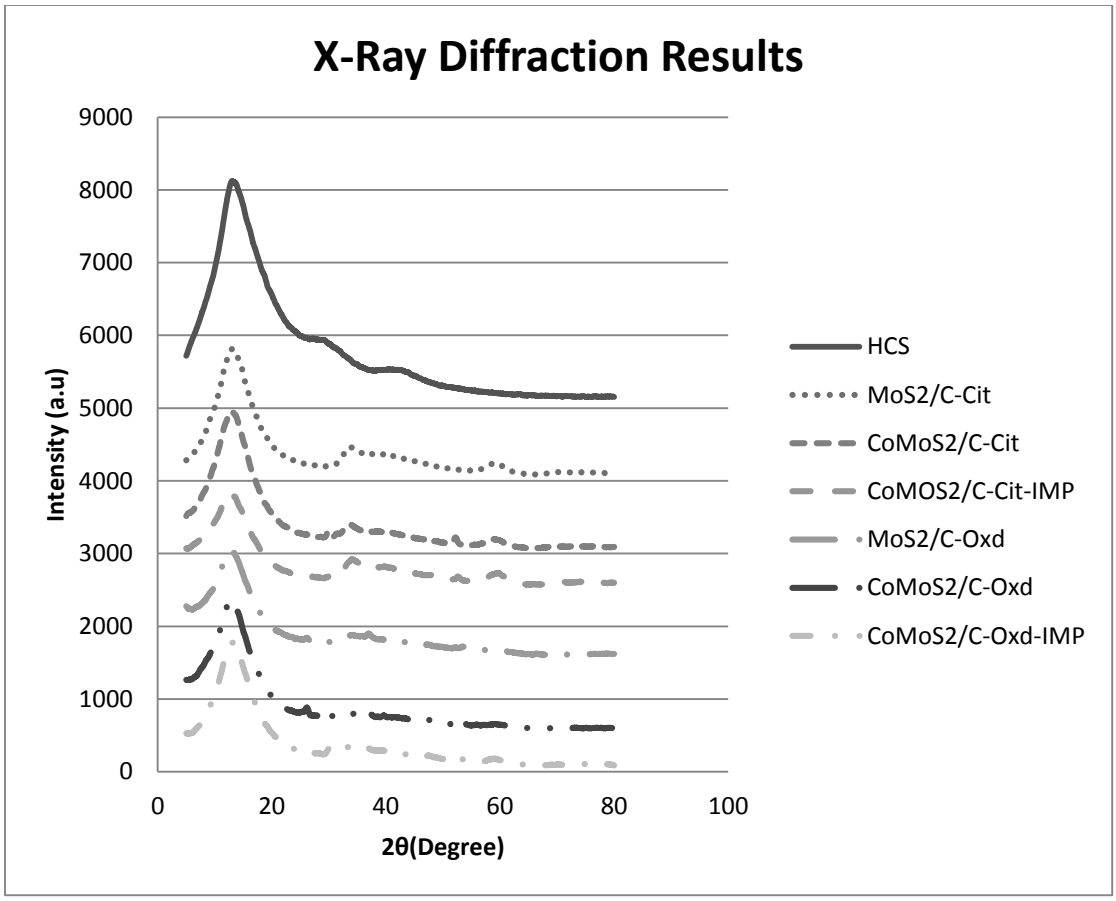

Figure 4.6 XRD Pattern of Synthesized Catalysts

4.4 Nitrogen Adsorption/ Desorption and BET:

Nitrogen adsorption and desorption used to identify the porosity of sample and its size distribution. BET aims to explain the physical adsorption of gas molecules on a solid surface and serves as the basis for an important analysis technique for the measurement of the specific surface area of a material. The nitrogen isotherm curve(See Figures 4.7, 4.8 4.9) is a typical shape of type III isotherm that indicate a formation of multilayers of adsorbed gas on the surface . All catalysts show same shape except the (Co) MoS_2/C-Oxide, which shows stronger adsorption capacity. The BET analysis (Table 4.2) show higher surface area for citrate based catalysts. This is an evidence of added micro porosity because of nicking; also the results of pore volume are aligned with BET trend.

Table 4.2 BET analysis of prepared catalysts

Catalyst Name	BET Surface area (m^2/g)	Pore Volume (cm^3/g)
MoS_2/C- oxide	182	0.1249
MoS_2/C- Cit	211	0.1357
$CoMoS_2$/C- oxide	180	0.1630
$CoMoS_2$/C- Cit	212	0.1554
$CoMoS_2$/C- oxide-IMP	130	0.1016
$CoMoS_2$/C- Cit-IMP	178	0.1207

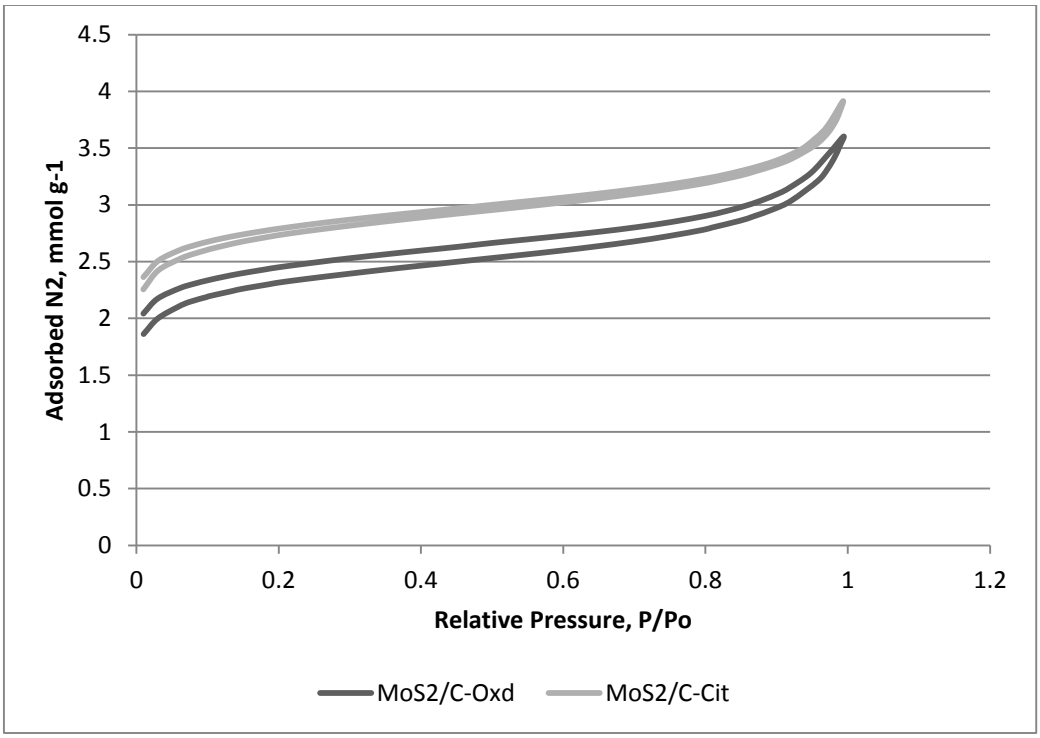

Figure 4.7 Nitrogen Adsorption/Desorption Isotherms of MoS_2/C-Oxide and MoS_2/C-Cit

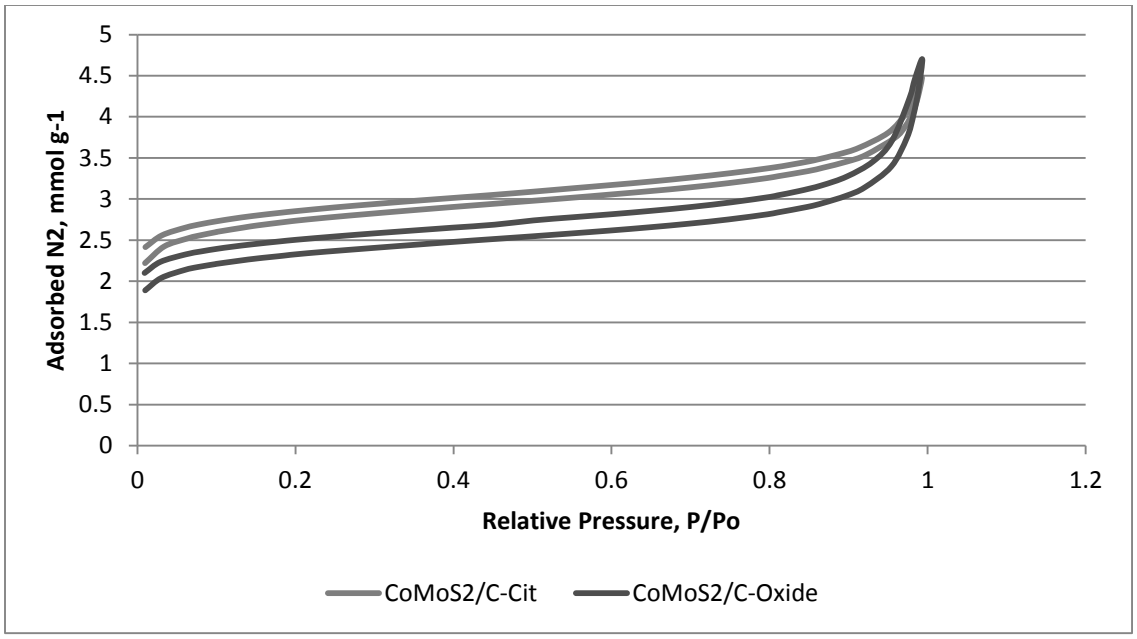

Figure 4.8 Nitrogen Adsorption/Desorption Isotherms of(Co) MoS_2/C-Oxide and (Co)MoS_2/C-Cit

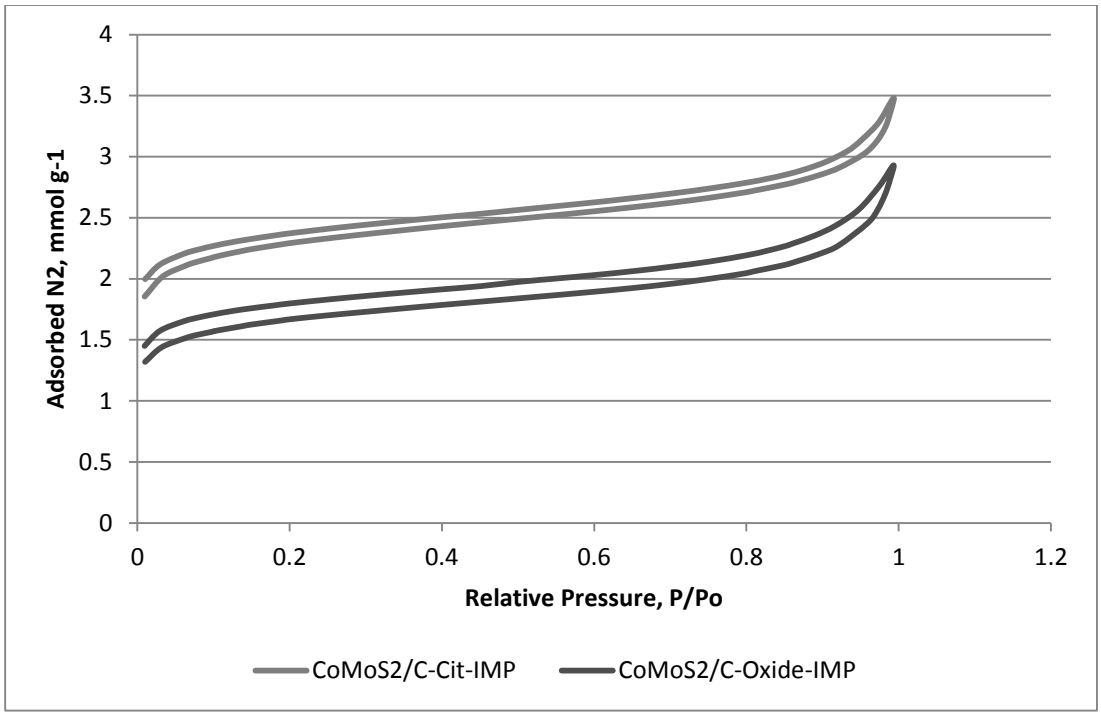

Figure 4.9 Nitrogen Adsorption/Desorption Isotherms of(Co) MoS_2/C-Oxide-IMP and (Co)MoS_2/C-Cit-IMP

4.5 Catalysts Activity

Six catalysts were synthesized using different precursors and synthesis routes in order to find the optimum catalyst for HDS of thiophenes. The catalysts are :

- MoS_2 / C- Oxide
- MoS_2 / C- CIT
- $CoMoS_2$ / C- Oxide
- $CoMoS_2$ / C- CIT
- $CoMoS_2$ / C- Oxide- IMP
- $CoMoS_2$ / C- CIT- IMP

MoS_2 / C were synthesized from molybdenum oxide or molybdenum citrate solutions. The reason is that citrate complex is hydrophobic and it is favored for bimetal system [31] Molybdenum sulfide catalysts were promoted with cobalt because it enhance the HDS activity of molybdenum sulfide catalysts by modifying the structure of active site and reduction in the required binding energy of thiophenes with active sites [32]. The activity of synthesized catalysts in the hydrodesulfurization (HDS) of dibenzothiophene (DBT) was studied using 4000ppm DBT dissolved in decane. The reaction was carried out at 320°C in stirred autoclave reactor at 4 MP pressure of Hydrogen for 3 hours. The yield versus percent of conversion of each catalyst in the hydrodesulfurization (HDS) of dibenzothiophene (DBT) are shown in figures 4.8 and 4.9. The reactions products are cyclohexylbenzene (CHB), biphenyl (BP) and tetrahydrodibenzothiophene (THDBT). In all the catalysts the yield of BP is generally higher than that of the CHB. Since it has already been established that BP is usually a product of direct desulfurization of DBT while CHB results from subsequent hydrogenation of partially hydrogenated DBT or BP, the

preponderance of BP over CHB is an early hint for the preference of these catalysts for DDS route. The yield of THDBT is generally increases to maximum and then decrease with reaction time indicating its intermediate.

0.02-0.03 g of elemental copper was added to the reaction vessel in order to scavenge H_2S and to minimize the inhibition effect of hydrogen sulfide (H_2S) because it found to suppress the reaction apparent rate of DDS route in the HDS of DBT [33].

4.5.1 Catalytic Activity of MoS_2/C-Oxide:

0.505g of MoS_2/C-Oxide and 0.029g of copper were add to 120 ml of decane solution containing 4000ppm DBT. The reaction mixture was pressurized to 4 MP and then heated to 320 ^oC. Samples were collected every 15 minutes in first two hours then every 30 minutes in the 3rd hour. The solution started with almost 100% DBT, 0.022164 M, and after 3 hours test the conversion of DBT found to be 68.44%. The products of reaction and DBT conversion are shown in fig 4.10. The composition of final mixture, according to Figure 4.10, was as follow: Cyclohexane (CyIH) 0.693%, Bicyclohexane (BCHY) 1.68% ,Cyclohexane-Benzene (CHB) 24.87%, Biphenyl (BP) 39.09%, Tetra and dihydrogenated dibenzothiophene (T+DHDBT) 2.31%, and dibenzothiophene (DBT) 31.36% .Concentration of BP, which is the product of DDS, is 1.57 times the concentration of CHB, which is the product of HYD route. This indicates the favoring of HDS through DDS route over HYD route. Same observation was reported in other literatures [34] that DDS is more favored when carbon is used as support. The concentration of benzene and cyclohexane are very small, this indicates that cracking and hydrogenation of HDS products is very small as a result of inert property of carbon support. Concentration of THDBT found to increase to maximum, $8.78x10^{-4}$ M, and then decrease with reaction time to $5.15x10^{-4}$M. This behavior indicates that TDHDBT is an intermediate product of HDS of DBT also the amount of TDHDBT is related to the activity of HYD route in the HDS of DBT [35].

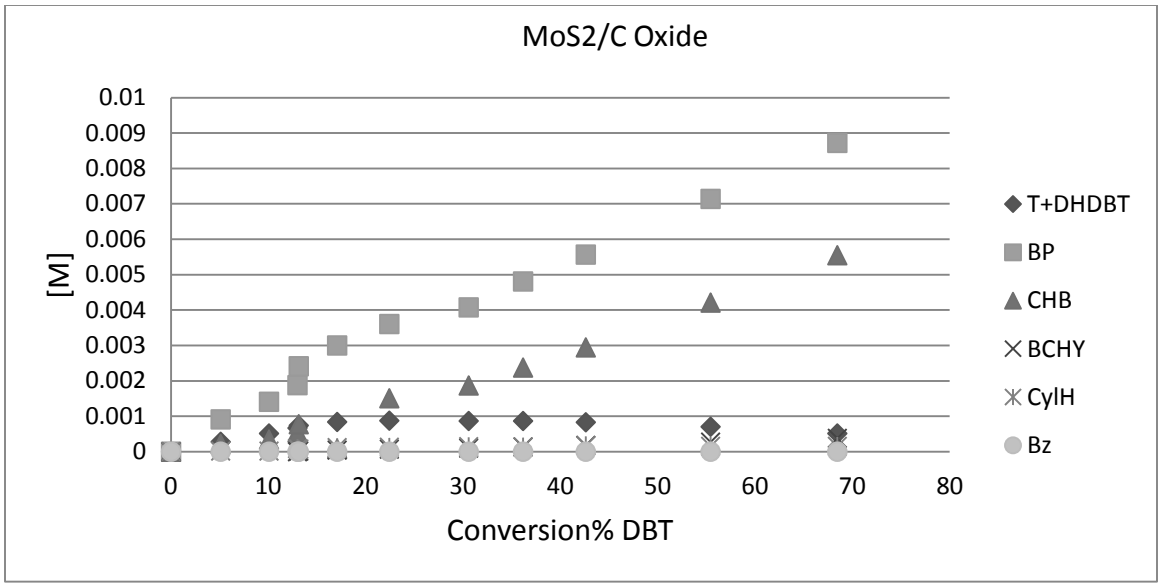

Figure 4.10 Products of HDS of DBT over MoS_2/C oxide.

4.5.2 Catalytic Activity of MoS_2/C-Cit:

0.51g of MoS_2/C-Oxide and 0.025g of copper were add to 120 ml of decane solution containing 4000ppm DBT. Once the reaction temperature reached, samples were collected every 15 minutes in first two hours then every 30 minutes in the 3rd hour. The solution started with almost 100% DBT, 0.02217 M, and after 3 hours test the conversion of DBT found to be 44.63%. The products of reaction and DBT conversion are shown in fig 4.11. The composition of final mixture, according to Figure 4.11, was as follows: Cyclohexane (CyIH) 0.541%, Bicyclohexane (BCHY) 0.461% ,Cyclohexane-Benzene (CHB) 13.53%, BiPhenyl (BP) 27.09%,Tetra and dihydrogenated dibenzothiophene (T+DHDBT) 3.51%, and dibenzothiophene (DBT)54.86% .Concentration of BP, which is the product of DDS, is 2.00 times the concentration of CHB, which is the product of HYD route. This indicates the favoring of HDS through DDS route over HYD route. Also the selectivity toward DDS is higher than MoS_2/C-Oxide, and it was noticed that conversion of DBT was slow in the first 2 hours but increased rapidly in the last hour of the test and over all conversion of DBT is less than MoS_2/C-Oxide. The reason for less DBT conversion is direct related to the lower molybdenum content in MoS_2/C-Cit compared to MoS_2/C-Oxide, 12.6 and 18.3% respectively. The slower conversion of DBT in the early stage of the reaction was due to hydrogen sulfide inhibition effect and the influence of this inhibition was higher when compared to MoS_2/C-Oxide but the selectivity of DDS is higher than one of MoS2/C-Oxide. These two observations are related to the structure of molybdenum sulfide crystals. It is suggested that molybdenum sulfide crystals in MoS_2/C-Cit have more stacking layers comparing with MoS_2/C-Oxide. This leads to more edge sites where the DDS takes place [36].

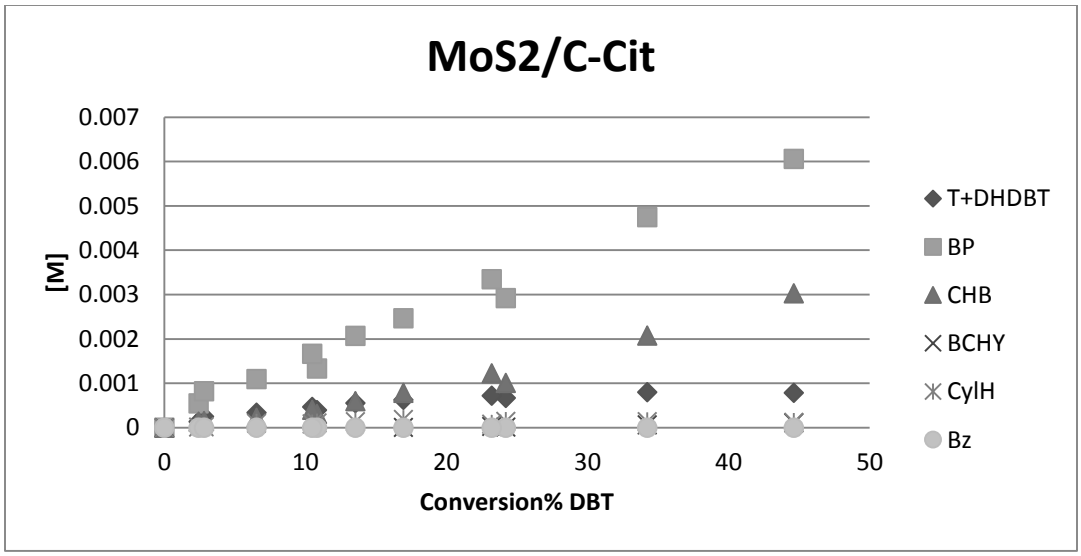

Figure 4.11 Products of HDS of DBT over MoS2/C oxide

4.5.3 Catalytic Activity of (Co)MoS_2/C-Oxide:

0.258g of (Co)MoS_2/C-Oxide and 0.032g of copper were add to 120 ml of decane solution containing 4000ppm DBT. Once the reaction temperature reached, samples were collected every 15 minutes in first two hours then every 30 minutes in the 3rd hour. The solution started with almost 100% DBT, 0.02159 M, and after 3 hours test the conversion of DBT found to be 54.89%. The products of reaction and DBT conversion are shown in fig 4.12. The composition of final mixture, according to Figure 4.12, was as follow: Cyclohexane (CyIH) 0.566%, Bicyclohexane (BCHY) 0.727% ,Cyclohexane-Benzene (CHB) 14.30%, Biphenyl (BP) 37.79%, Tetra and dihydrogenated dibenzothiophene (T+DHDBT) 1.93%, and dibenzothiophene (DBT)44.66%. Concentration of BP, which is the product of DDS, is 2.64 times the concentration of CHB, which is the product of HYD route. This indicates the favoring of HDS through DDS route over HYD route. Also it is more selective toward DDS than unprompted MoS_2/C-Oxide. (Co)MoS_2/C-Oxide was less influenced by hydrogen sulfide inhibition; this is because of availability of sulfur vacancies formed by coordination of Co-Mo-S and make the HDS reaction more rapid [32]. The less conversion of DBT in (Co) MoS2/C-Oxide is because of using lower amount of catalyst compared with unprompted MoS_2/C-Oxide.

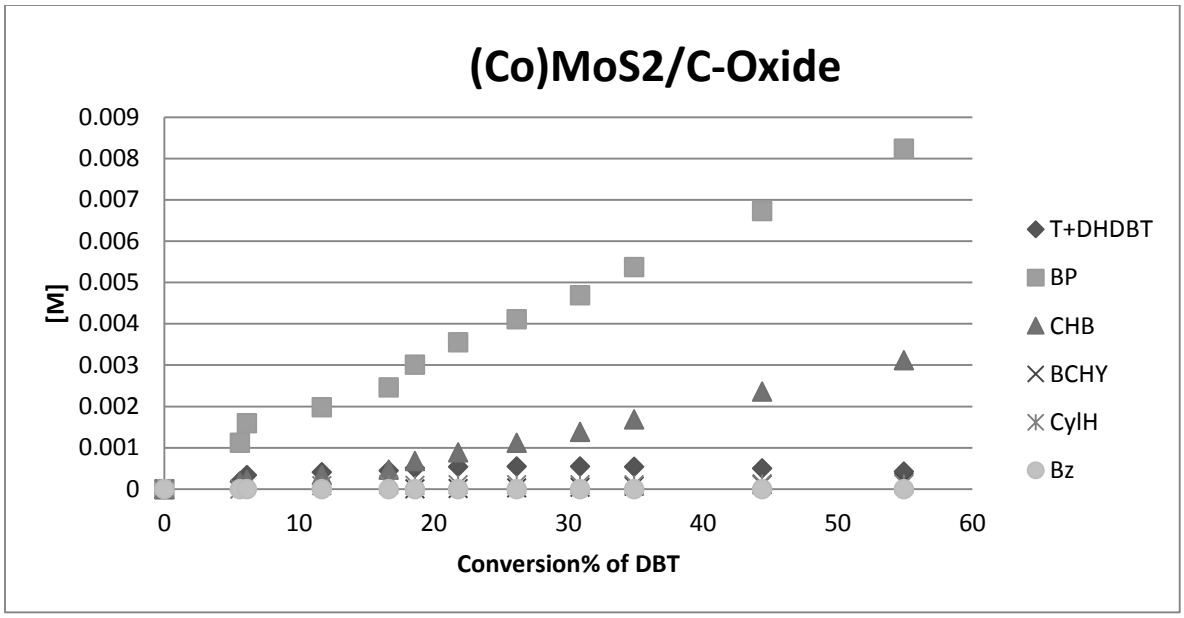

Figure 4.12 Products of HDS of DBT over (Co)MoS_2/C Oxide

4.5.4 Catalytic Activity of (Co)MoS_2/C-Cit:

0.256g of (Co)MoS_2/C-Cit and 0.032g of copper were add to 120 ml of decane solution containing 4000ppm DBT. Once the reaction temperature reached, samples were collected every 15 minutes in first two hours then every 30 minutes in the 3rd hour. The solution started with almost 100% DBT, 0.02159 M, and after 3 hours test the conversion of DBT found to be 54.89%. The products of reaction and DBT conversion are shown in figure 4.13. The composition of final mixture, according to Figure 4.12, was as follow: Cyclohexane (CyIH) 1.04%, Bicyclohexane (BCHY) 0.60% ,Cyclohexane-Benzene (CHB) 11.74%, Biphenyl (BP) 37.22%,Tetra and dihydrogenated dibenzothiophene (T+DHDBT) 1.95%, and dibenzothiophene (DBT)48.67% .Concentration of BP, which is the product of DDS, is 3.17 times the concentration of CHB, which is the product of HYD route. This indicates the favoring of HDS through DDS route over HYD route. Also it is more selective toward DDS than unprompted MoS_2/C-Cit. Concentration of THDBT is found to increase to maximum and then decrease with reaction time indicating its intermediate nature. Hydrogen sulfide inhibition effect was observed, however to lesser extent compared to MoS_2/C-Cit but still higher when compared to (Co)MoS_2/C-Oxide. It is following the same trend as catalyst synthesized with Citric acid. This indicates that stacking of molybdenum sulfide edge layers is higher in the catalyst than (Co)MoS_2/C-Oxide. This is confirmed by the products of HDS of DBT and the XRD pattern. The conversion of DBT in (Co)MoS_2/C-Cit more than (Co)MoS_2/C-Oxide. This is consistent with the elemental analysis results in Table 4.1, where the (Co)MoS_2/C-Oxide have higher metals loading than (Co)MoS_2/C-Cit.

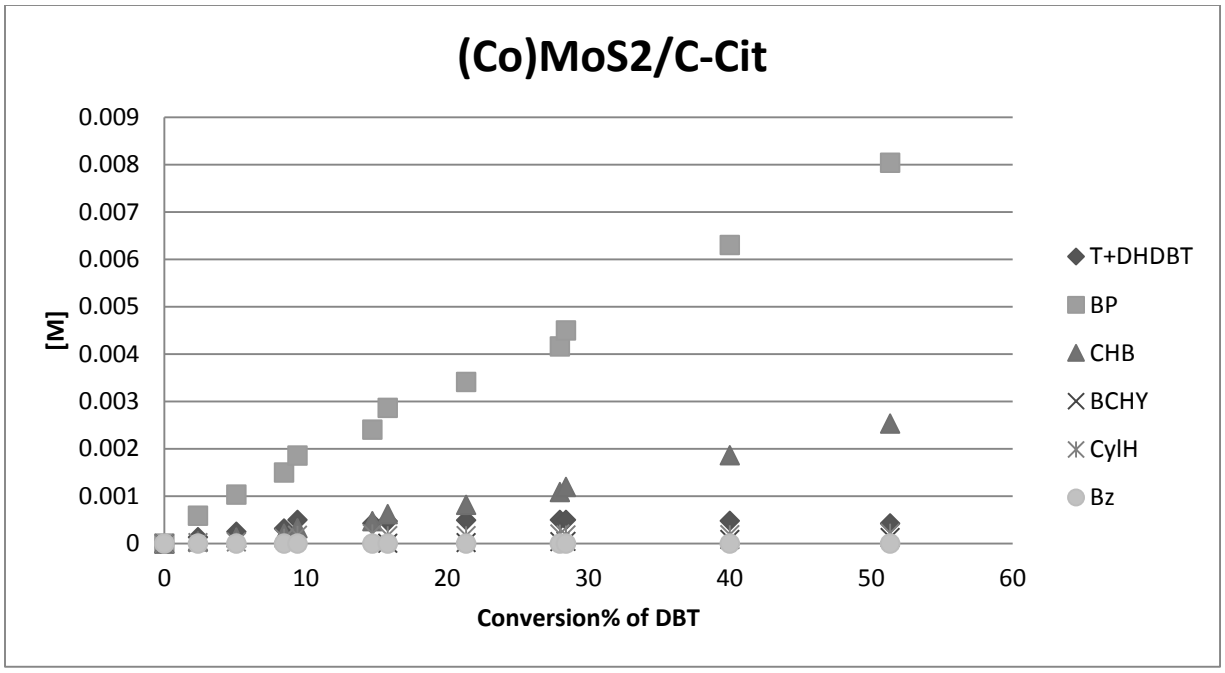

Figure 4.13 Products of HDS of DBT over (Co)MoS_2/C Oxide

4.5.5 Catalytic Activity of (Co)MoS_2/C-Cit -IMP:

0.51g of (Co)MoS_2/C-Cit -IMP and 0.025g of copper were add to 120 ml of decane solution containing 4000ppm DBT. Once the reaction temperature reached, samples were collected every 15 minutes in first two hours then every 30 minutes in the 3rd hour. The solution started with almost 100% DBT, 0.02287 M, and after 3 hours test the conversion of DBT found to be 69.75%. The products of reaction and DBT conversion are shown in figure 4.14. The composition of final mixture, according to Figure 4.14, was as follow: Cyclohexane (CyIH) 0.657%, Bicyclohexane (BCHY) 0.572% ,Cyclohexane-Benzene (CHB) 20.36%, Biphenyl (BP) 46.91%,Tetra and dihydrogenated dibenzothiophene (T+DHDBT) 1.54%, and dibenzothiophene (DBT)29.95% .Concentration of BP, which is the product of DDS, is 2.3 times the concentration of CHB, which is the product of HYD route. This indicates the favoring of HDS through DDS route over HYD route. But the DDS selectivity is less comparing with (Co)MoS_2/C-Cit. two possible reasons for the observation: first, phase separation of cobalt is higher in (Co)MoS_2/C-Cit-IMP as shown in the XRD pattern, second the stacking of molybdenum sulfide is less presenting less available sites for DDS. The conversion of DBT in the catalyst synthesized via impregnation route is higher than that prepared by co precipitation because of higher active metals loading as per literature [34] that cobalt promoted molybdenum sulfide synthesized by subsequent sulfidation is more active than simultaneously sulfide that cobalt promoted molybdenum sulfide.

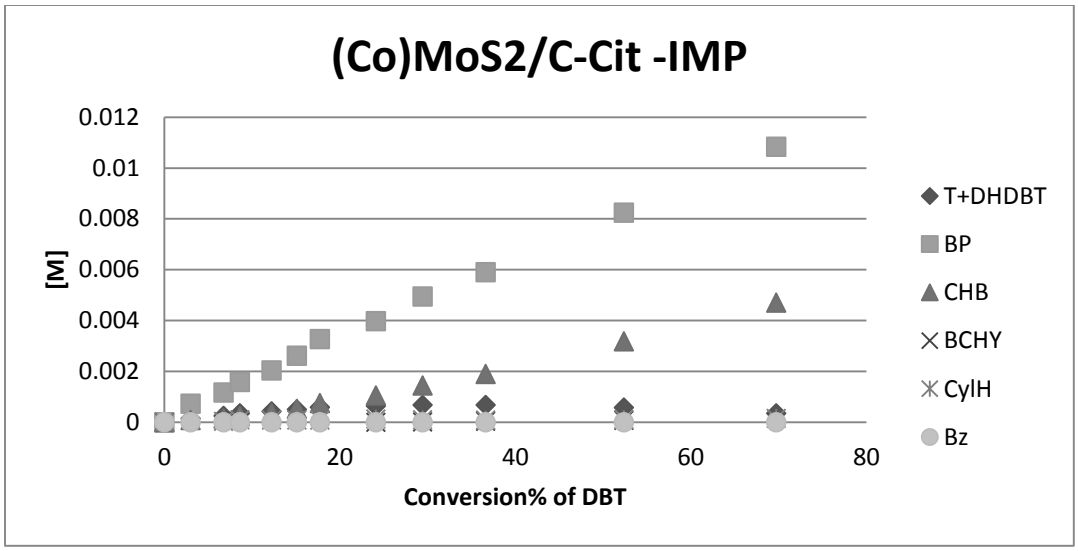

Figure 4.14 Products of HDS of DBT over (Co)MoS_2/C-Cit-IMP

4.5.6 Catalytic Activity of (Co)MoS_2/C-Oxide -IMP:

0.51g (Co)MoS_2/C-Oxide -IMP and 0.025g of copper were add to 120 ml of decane solution containing 4000ppm DBT. Once the reaction temperature reached, samples were collected every 15 minutes in first two hours then every 30 minutes in the 3rd hour. The solution started with almost 100% DBT, 0.02287 M, and after 3 hours test the conversion of DBT found to be 69.75%. The products of reaction and DBT conversion are shown in figure 4.15. The composition of final mixture, according to Figure 4.15, was as follows: Cyclohexane (CyIH) 0.657%, Bicyclohexane (BCHY) 0.572% ,Cyclohexane-Benzene (CHB) 20.36%, Biphenyl (BP) 46.91%,Tetra and dihydrogenated dibenzothiophene (T+DHDBT) 1.54%, and dibenzothiophene (DBT)29.95% .Concentration of BP, which is the product of DDS, is 2.08 times the concentration of CHB, which is the product of HYD route. It is less selective toward DDS than (Co) MoS_2/C-Oxide and (Co)MoS_2/C-Cit-IMP. Also the effect of Hydrogen Sulfide inhibition is less compared to both (Co) MoS_2/C-Oxide and (Co)MoS_2/C-Cit-IMP and it is consistent with observations form previous catalysts. The conversion of DBT over the catalyst synthesized via the impregnation route is higher than that prepared via co precipitation because of higher active metals loading. Also the inhibition effect of hydrogen sulfide is less compared to that of (Co)MoS_2/C-Cit –IMP[34]. Unlike previous catalysts, (Co)MoS_2/C-Cit-IMP and (Co)MoS_2/C-Oxide-IMP show same conversion of DBT. Although that molybdenum content is much less in (Co)MoS_2/C-Cit-IMP compared to (Co)MoS_2/C-Oxide-IMP, the cobalt content in (Co)MoS_2/C-Cit-IMP is 4 times higher than (Co)MoS_2/C-Oxide-IMP, see table 4.1. It is obvious that cobalt in (Co)MoS_2/C-Cit-IMP decorated in the molybdenum sulfide structure and exhibited less phase separation. This observation reflects the role of citric acid in shaping the structure of cobalt promoted molybdenum sulfide and increase the formation of Co-Mo-S phase [31].

4.6 Kinetic Treatment

Based on the results obtained from the reaction analyses in section 4.5, the proposed reaction mechanism and network for the hydrodesulfurization (HDS) of dibenzothiophene

(DBT) is given in Figure 4.16. According to the scheme, HDS of DBT may occur via two parallel paths: initially it may be hydrogenated to yield THDBT which is then desulfurized to CHB and subsequently hydrogenated further to BCH. The other route is the direct desulfurization to produce BP, which could then be hydrogenated to CHB. Cyclohexylbeneze (CHB) is then hydrogenated to produce BCH.

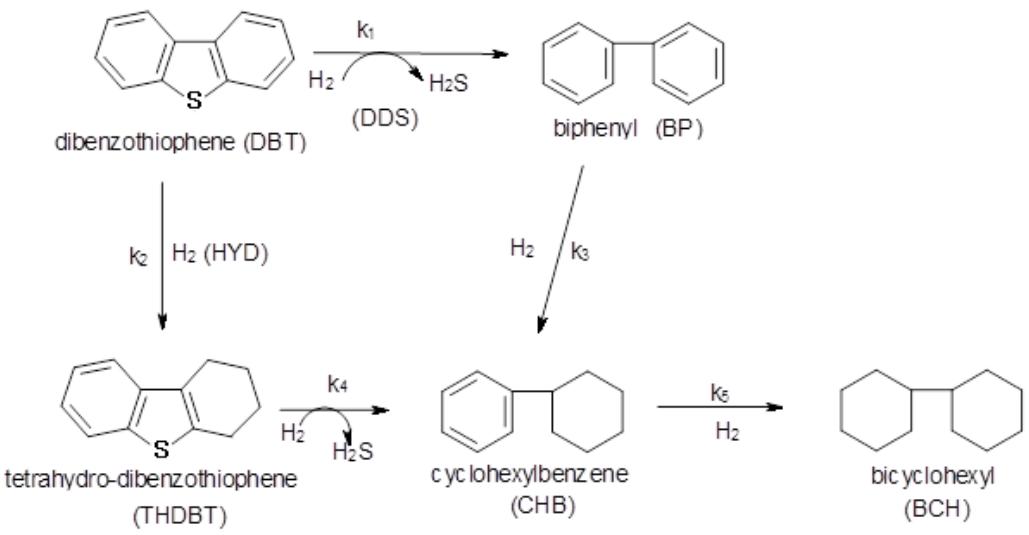

Figure 4.15 Proposed reaction network for the HDS of DBT

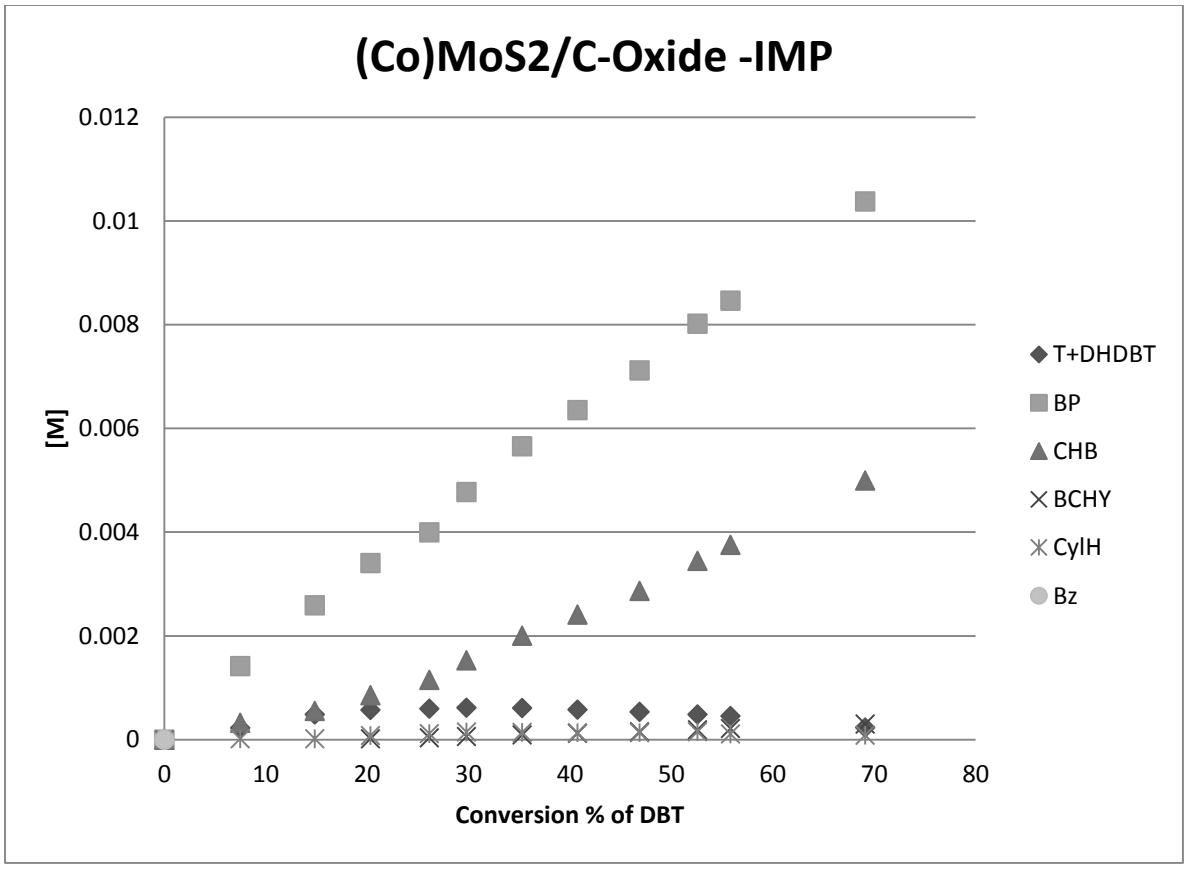

Figure 4.16 Products of HDS of DBT over (Co)MoS_2/C-Oxide-IMP

Considering the hydrodesulfurization reaction conditions used in this study, the following assumptions have been made [35]:

1. The hydrogen concentration remains constant throughout the reaction since it was fed in excess.
2. HDS of individual sulfur compounds follow pseudo-first order kinetics
3. The inhibition effect of the products of HDS of DBT is considered negligible except the effect of H_2S inhibition.
4. The effect of H_2S was neutralized by addition of Cu powder to the reaction mixture.

In order to verify the proposed mechanism presented in Figure 4.16, the kinetic equations that fit the experimental data obtained in HDS of DBT based on Langmuir-Hinshelwood (L-H) type equation with two kinds of catalytic active sites were developed.

Accordingly, the overall rate can be expressed by two parts:

$$R_{DDS} = \frac{k_1 K_1 C_{DBT}}{1 + K_1 C_{DBT} + \cdots} \qquad (1)$$

$$R_{HYD} = \frac{k_2 K_2 C_{DBT}}{1 + K_1 C_{DBT} + \cdots} \qquad (2)$$

Here, R_{DDS} and R_{HYD} are the rate of direct desulfurization (DDS) and the rate of hydrogenation (HYD) of DBT, respectively. K_1, k_1 and K_2, k_2 are the equilibrium adsorption constants of DBT over the catalytic active sites and the reaction rate constants for DDS and HYD, respectively, as shown in Figure 4.16. C_{DBT} is the concentration of DBT at a given reaction time.

Under the reaction conditions used, the rate equations (1and 2) reduce to pseudo-first order equations where the overall rate, R_{total} can be taken as the sum of the rate of direct desulfurization (DDS) and the rate of hydrogenation (HYD):

$$R_{total} = (k_1K_1 + k_2K_2)C_{DBT} \quad (3)$$

$$R_{total} = k_0C_{DBT} \quad (4)$$

Where $k_0 = (k_1K_1 + k_2K_2)$ is taken as the apparent rate constant of the DBT conversion. By considering every component of the reaction network, the material balance equations (of a batch reactor) of all the components of the reaction network (Fig 4.16) can be written as follow:

$$\frac{dC_{DBT}}{dt} = k_0C_{DBT} \quad (5)$$

$$\frac{dC_{BP}}{dt} = k_1C_{DBT} - k_3C_{BP} \quad (6)$$

$$\frac{dC_{THDBT}}{dt} = k_2C_{DBT} - k_4C_{THDBT} \quad (7)$$

$$\frac{dC_{CHB}}{dt} = k_4C_{BP} - k_5C_{THDBT} \quad (8)$$

Where k_1, k_2, k_3 and k_4 are the apparent rate constants of the respective steps in the reaction network in Figure 4.16. Solutions of these differential equations (5-7) are the following expressions:

$$C_{DBT} = C^0_{DBT}e^{-k_0t} \quad (10)$$

$$C_{BP} = C^0_{BP}e^{-k_3t} + \frac{C^0_{DBT}k_1}{k_3 - k_0}[e^{-k_0t} - e^{-k_3t}] \quad (11)$$

$$C_{THDBT} = C^0_{THDBT}e^{-k_4t} + \frac{C^0_{DBT}k_2}{k_4 - k_0}[e^{-k_0t} - e^{-k_4t}] \quad (12)$$

WhereC^0_{DBT}, C^0_{BP}, C^0_{THDBT} are the concentrations at reaction time t=0 of the DBT, BP, and THDBT respectively.

4.7 Model Reaction Fitting

Computational analyses were carried out using Mathematica 5.0 to fit the experimental data with Langmuir-Hinshelwood (L-H) equations. Kinetic parameters were generated at a correlation factor of greater than 95% between experimental and calculated data. Figures 4.19 show the comparisons between experimental and calculated concentrations for the reaction at 320°C over catalyst with CoMoS2/ C- Oxide-IMP. Interestingly, in all the fittings, we obtained very good correlation between the experimental and theortical data. For the DBT curve, Figure 4.18 , the concentration of DBT decreases exponentionally with reaction time in accordance with kientic of pusedo-first order conversion. Figures 4.17 also displays the fitting curves for the other products. Although, in all, there are good agreements between experimental and the calculated data, a slight deviation is noticed for the THDBT curve[33]. The reactions' rate constants for all catalysts are shown in table 4.3. It's noticed that CoMo/C-Oxd-Imp catalysts has exhibited the highest acivity among the set of catalysts used where, according to Table 4.3, the CoMo/C-Oxd-Imp catalysts had the largest rate constants for all of the reaction steps shown in Fighure 4.18. In addition, the addition of Co has increased the rate of direct desulfurization relative to that of the hydrogenation route, where k_1/k_2 values were nearly similar for all Co containig samples and larger than that of samples containing MoS_2 only. Moreover, the sample CoMo/C-Cit-Imp exhibited the largest k_1/k_2 ratio, which according to the rim-edge model, must have the largest crystals and number of stacks, which is also in line with the XRD results.

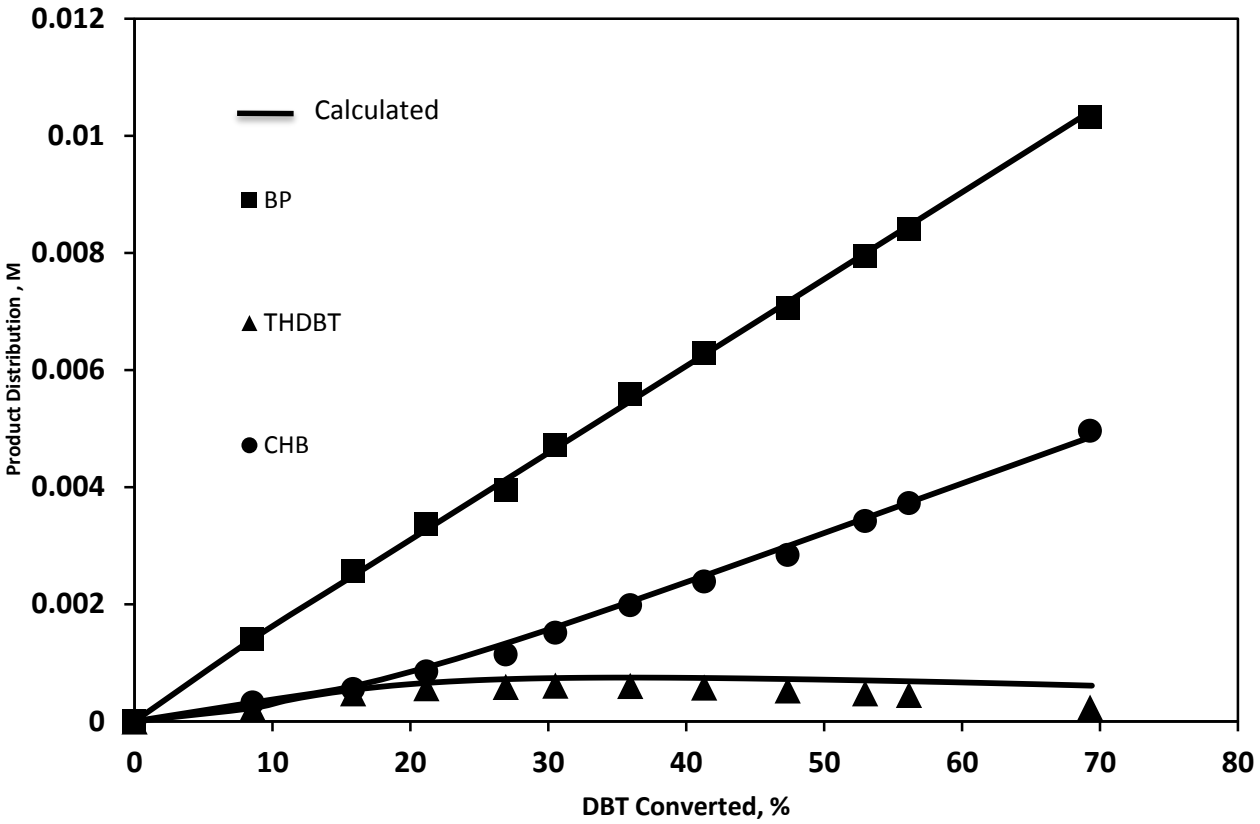

Figure 4.17 Product Selectivity vs. conversion of DBT at 320°C for $CoMoS_2$/ C- Oxid-IMP

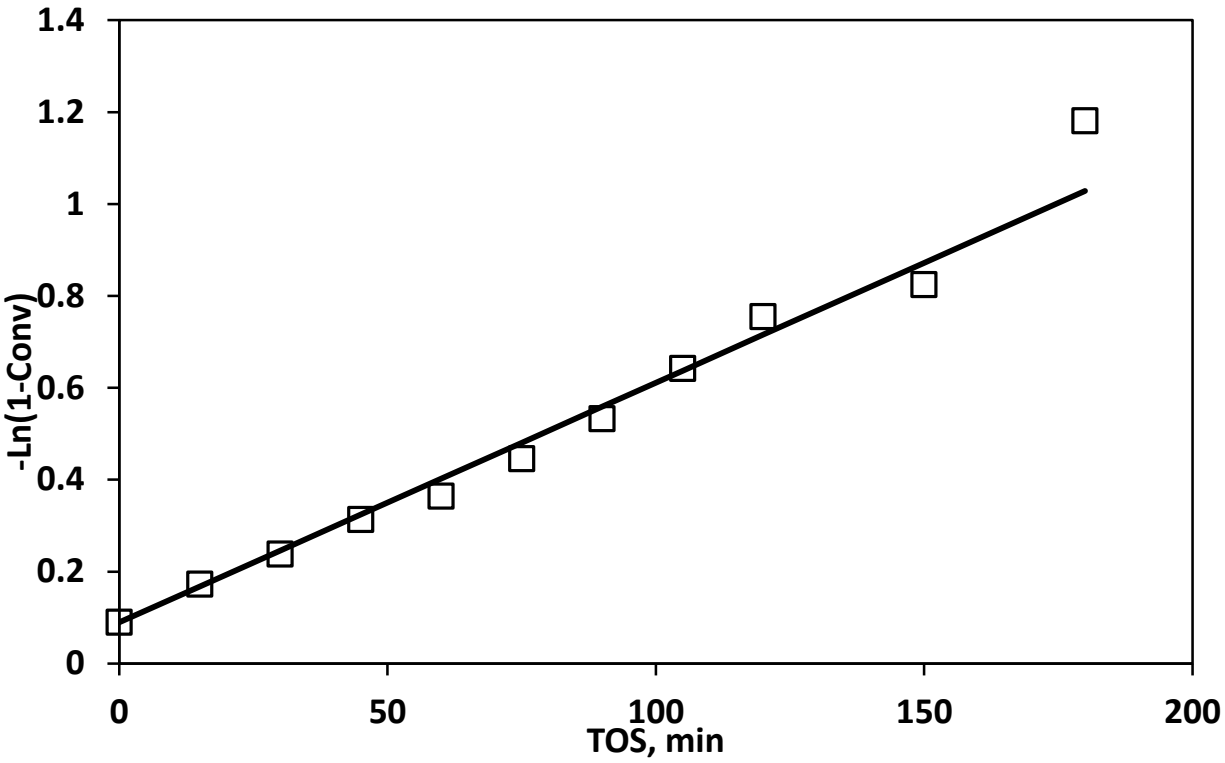

Figure 4.18 Pseudo-first order plot of the HDS of DBT over $CoMoS_2$/ C- Oxide-IMP

Table 4.3 overall and individual apparent rate constants for the HDS of DBT at 320°C (10^{-3}/min)

Sample	k_o/min	k_1/min	k_2/min	k_3/min	k_4/min	k_5/min	k_1/k_2
CoMo/C-Cit-Imp	2.812	2.042	0.77	0	20.495	13.265	2.653799
CoMo/C-Oxd-Imp	5.217	3.385	1.832	0	46.125	49.025	1.847917
CoMo/C-Cit	2.926	1.92	1.006	0	16.129	10.748	1.907824
CoMo/C-Oxd	2.952	2.006	0.946	0	22.106	18.601	2.120776
MoS2/C-Cit	1.952	1.07	0.882	0	14.361	12.558	1.213413
MoS2/C-Oxd	3.607	2.035	1.572	0	18.725	11.209	1.294991

4.8 Catalyst evaluation by desulfurization of model FCC gasoline using microreactor:

The above catalysts were also evaluated for desulfurization of thiophene in FCC model gasoline stream. The composition of FCC model gasoline was as follow: (3% 2-Methyl Thiophene, 20% 2,3 di methyl but2-ene, 40% o-xylene 47% n-heptane). Figure 4.19 and Figure 4.20 show the results of Model FCC Gasoline desulfurization. The prepered catalysts show lower Hydrodesulfurization performance comparing with standard cobalt molymbdenum supported on alumina.Also the rate of hydrogenation was lower but it is an advantage because the olefin content is higer in the product, hence higher ocatne number. The results of HDS of model FCC gasoline are not consistent with avilable litrautres where the carbon supported (Co)MoS_2 show better performance than commercial (Co)MoS_2 supported on alumina [34] . The main reason is that catalyst were partially promoted by cobalt and some of cobalt formed separate sulfide phase of Co_9S_8 , which is not active in HDS. The curves of reaction rate are consistent with the amount of active metals. Also citrate based catalyst showed lower performance than oxide based catalysts in HDS of 2-MT . like the HDS of DBT, citrate based catalysts were more affected by hydreogen sulfide inhibition than oxide based catalysts. But is show similar perofrmance in hydrogenation of 2,3 DM2B because brim sites are less affected by hydrogen sulfide inhibition[33].

The condtions of reaction were as follow:

- Catalyst weight= 1.49 g
- Reaction temp= 225 C
- Reaction Pressure = 20 bar
- H2 Flow rate = 20 ml/min
- WHSV=3 /h
- HC Feed flow = 0.1 ml/min
- H2/HC= 200 l/l

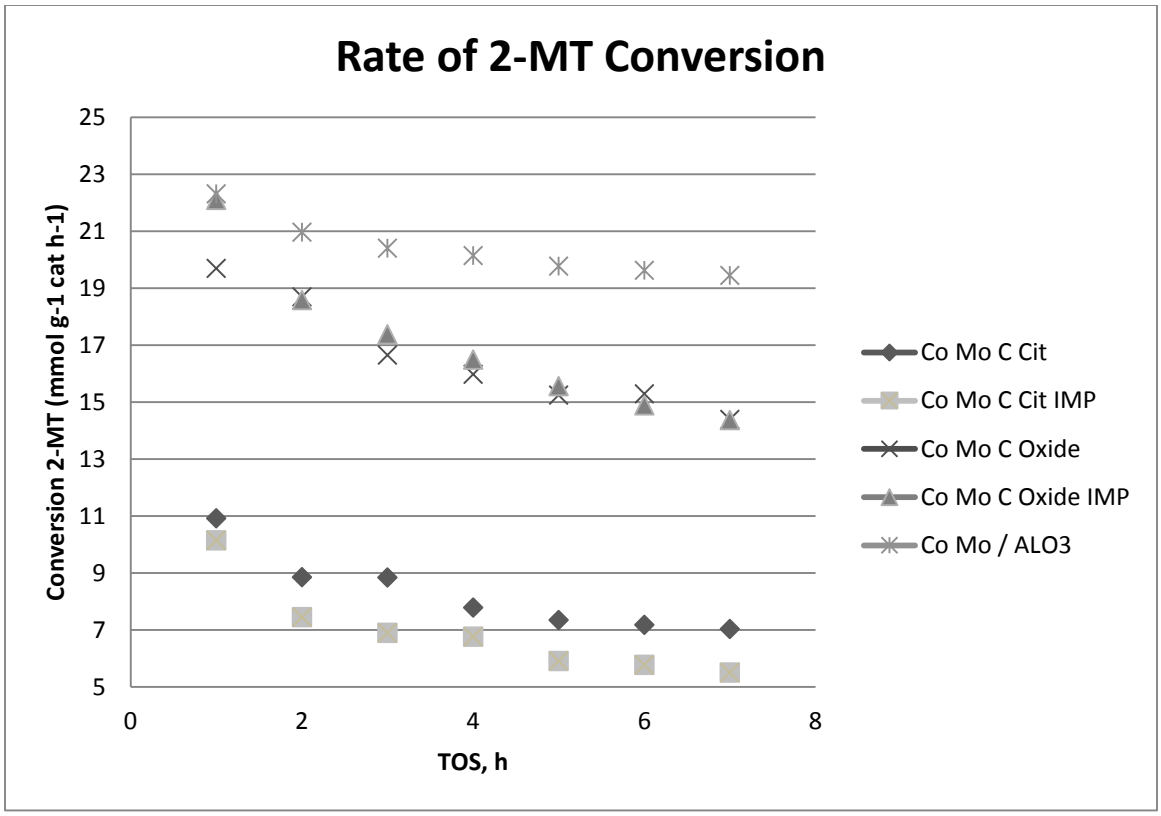

Figure 4.19 Performance of Synthesized catalyst in hydrodesulfurization of 2-MT in Model FCC-Gasoline

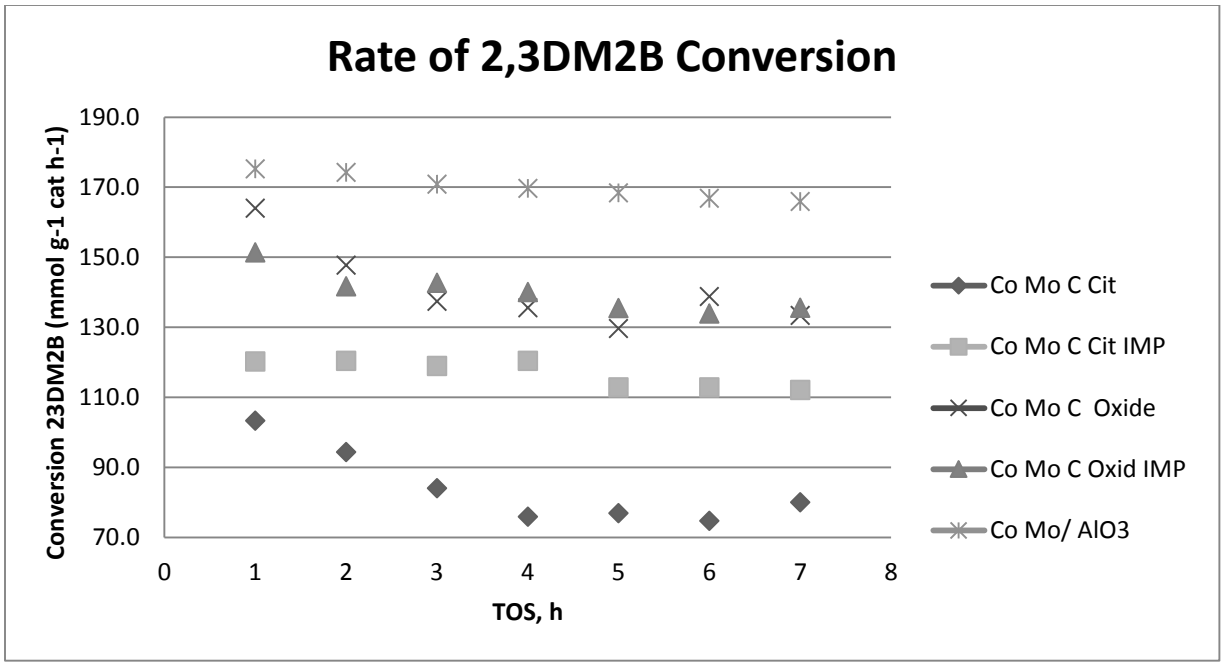

Figure 4.20 Performance of Synthesized catalyst in hydrogenation of 2,3DM2B in Model FCC-Gasoline

CHAPTER 5

Conclusion and Recommendations

5.1 Conclusion:

The (Co)MoS_2 HDS catalysts supported on hollow carbon sphere were synthesized successfully. The following are the summery of our investigation:

1- The catalysts showed higher selectivity of DDS route over HYD route in HDS of DBT.
2- Oxide based catalyst showed better performance comparing with Citrate based. This due to higher loading capacity of active metal on oxide base route.
3- Citrate based catalysts show higher selectivity of DDS route in HDS of DBT because of larger stacking of molybdenum sulfide.
4- The activity of catalysts in overall HDS reactions was less than commercial $CoMoS_2$/ Alumina. This is because of low loading of active metals.
5- Catalysts synthesized by simultaneous precipitation show the highest conversion per unit mass of catalyst and highest selectivity of DDS in HDS of DBT.

5.2 Recommendations:

1- Optimize the ratio of resorcinol and formaldehyde to avoid excessive nicking in hollow carbon sphere.

2- Study the effect of citric acid and the structure of molybdenum sulfide crystals.

3- Optimize the required amount of citric acid in order to minimize the excessive carbon in formation of hollow carbon spheres

4- Study the catalyst with XPS and TEM to build better understanding of the structure.

5- Use different promoting metals to enhance the catalysts performance.

References

[1] M. Breysse, G. Djega-Mariadassou, S. Pessayre, C. Geantet, M. Vrinat, G. Perot, M. Lemaire, Deep desulfurization: reactions, catalysts and technological challenges, Catal. Today 84 (2003) 129.

[2] I.V. Babich, J.A. Moulijn, Science and technology of novel processes for deep desulfurization of oil refinery streams: a review, Fuel 82 (2003) 607.

[3] (a) C. Song, An overview of new approaches to deep desulfurization for ultra-clean gasoline, diesel fuel and jet fuel, Catal. Today 86 (2003) 211-263.
(b) C. Song, X. Ma, New design approaches to ultra-clean diesel fuels by deep desulfurization and deep dearomatization, Appl. Catal. B: Environ. 41 (2003) 207.

[4] I. Vergov, I. Shishkova, Catalyst advances promote production of near zero sulphur diesel, Petrol. Coal 51 (2009) 136–139.

[5] Whitehurst, D.D., Isoda, T., & Mochida, I., Present state of the art an future challenges in the hydrodesulfurization of polyaromatic sulfur compounds (1998). *Adv. Catal. 42*, 345-471.

[6] A. Stanislaus, A. Marafi, M. S. Rana, Recent advances in the science and technology of ultra low sulfur diesel (ULSD) production, Catalysis Today 153 (2010) 1-68.

[7] Fusheng Ouyang, Xu Pei, Xuhong Zhao, & Huixin Weng, Effect of Operation Conditions on the Composition and Octane Number of Gasoline in the Process of Reducing the Content of Olefins in Fluid Catalytic Cracking (FCC) Gasoline, Energy& Fuels 24 (2010) 475-482

[8] T. Fujikawa, H. Kimura, K. Kiriyama, K. Hagiwara, Development of ultra-deep HDS catalyst for production of clean diesel fuels, Catal. Today 111 (2006) 188–193.

[9] Topsoe hydrotreating catalysts: http://www.topsoe.com/products/ CatalystPortfolio.aspx.

[10] S. Torrisi, The challenging chemistry of ultra-low sulfur diesel. Process Technology, Catalysis, World Refining. December, 2002 (http://www.shell.com/static/criterion-gb/downloads/pdf/trade pub reprints/wr 1201reprinttorrisi ulsd.pdf).

[11] R. Shafi, G.J. Hutchings, Hydrodesulfurization of hindered dibenzothiophenes: an overview, Catal. Today 59 (2000) 423–442.

[12] T. Kabe, A. Ishihara, Q. Zang, Deep desulfurization of light oil. Part 2: hydrodesulfurization of dibenzothiophene, 4-methyldibenzothiophene and 4,6-dimethyldibenzothiophene, Appl. Catal. A 97 (1993) L1–L9.

[13] M. J. Girgis, B.C. Gates, Reactivities, reaction networks and kinetics in high pressure catalytic hydroprocessing, Ind. Eng. Chem. Res. 30 (1991) 2021–2058.

[14] B.C. Gates, H. Topsoe, Reactivities in deep catalytic hydrodesulfurization: challenges, opportunities, and the importance of 4-methyldibenzothiophene and 4,6 dimethyldibenzothiophene, Polyhedron 16 (1997) 3213–3217.

[15] K. P. de Jonge (editor), Synthesis of solid catalysts, Wiley publication, pp. 301-328.

[16] Candia, R., Sorensen, O., Villadsen, J., Topsoe, N., Clausen, B.S., & Topsoe, H. (1984). *Bull. Soc. Chim. Belg. 93*, 763.

[17] B. Shen, H. Li, W. Zhang, Y. Zhao, Z. Zhang, X. Wang, S. Shen, A novel composite support for hydrotreating catalyst aimed at ultra-clean fuels, Catal. Today 106 (2005) 206–210.

[18] M. J. Vissenberg, Y. van der Meer, E.J.M. Hensen, V.R.J. de Beer, A.M. van der kraan, R.A. van Santen, J.A.R. van veen, The effect of support interaction on the sulfidability of Al2O3 and TiO2 supported CoW and NiW hydrodesulfurization catalysts, J. Catal. 198 (2001) 151–163.

[19] J. P. R. Vissers, B. Scheffer, J.H.J. de Beer, J.A. Moulijh, R. Prins, Effect of the support on the structure of Mo-based hydrodesulfurization catalysts activated carbon versus alumina, J. Catal. 105 (1987) 277-284.

[20] R. G. Lehveld, A.J. van Dillen, J.W. Geus, D.C. Komgsberger, A Mo–K edge XAFS study of the metal sulfide–support interaction in (Co)Mo supported alumina and titania catalysts, J. Catal. 165 (1997) 184–196.

[21] Breysse, M., Portefaix, J.-L., & Varinat, M. (1991). *Catal. Today 10*, 489.

[22] Hubert-pfalzgraf, L. G. *New J. of Chem.* **1987**, *11*, 663.

[23] Guglielmi, M.; Carturan, G. *J. Non-Cryst. Solids* **1988**, *100*, 16.

[24] Vikreva, O.; Kalinina, O.; Kumacheva, E. *Adv. Mater.* **2000**, *12*, 110.

[25] An-Hui Lu, Guang-Ping Hao, Qiang Sun, Xiang-Qian Zhang, Wen-Cui Li, Chemical Synthesis of Carbon Materials With Intriguing Nanostructure and Morphology, *Macromol. Chem. Phys.* **2012**, *213*, 1107−1131

[26] Neil J. Coville , Sabelo D. Mhlanga Edward N. Nxumalo, Ahmed Shaikjee, A review of shaped carbon nanomaterials, S Afr J Sci 2011; 107(3/4)

[27] William S. Cooke, Eckhardt Schmidt, Chunshan Song, and Harold H. Schobert, Reactions of Dibenzothiophene with Hydrogen in the Presence of Selected Molybdenum, Iron, and Cobalt Compounds, *Energy & Fuels* **1996,** *10*, 591-596

[28] Fusheng Ouyang, Xu Pei, Xuhong Zhao, and Huixin Weng, Effect of Operation Conditions on the Composition and Octane Number of Gasoline in the Process of Reducing the Content of Olefins in Fluid Catalytic Cracking (FCC) Gasoline, Energy Fuels 2010, 24, 475–482

[29] Hamdy Farag, Kinetic Analysis of the Hydrodesulfurization of Dibenzothiophene Approach Solution to the Reaction Network, *Energy & Fuels* 2006, *20*, 1815-1821

[30] E. J. M. Hensen, M. J. Vissenberg, V. H. J. de Beer, J. A. R. van Veen, and R. A. van Santen, Kinetics and Mechanism of Thiophene Hydrodesulfurization over Carbon-Supported Transition Metal Sulfides, Journal of Catalysis (1996)163, 429–435

[31] Nino Rinaldi, Tekeshi Kubota, and Yasuaki Okamoto**,** Effect of Citric Acid Addition on Co-Mo/B2O3/Al2O3 Catalysts Prepared by a Post-Treatment Method. *Ind. Eng. Chem. Res.* 2009**,** *48*, 10414–10424

[32] Poul Georg Moses , Berit Hinnemann , Henrik Topsøe , Jens K. Norskøv, The effect of Co-promotion on MoS2 catalysts for hydrodesulfurization of thiophene: A density functional study, Journal of Catalysis (2009) 268, 201–208

[33] Hamdy Farag, Investigation of the Influence of H_2S on Hydrodesulfurization of Dibenzothiophene over a Bulk MoS_2 Catalyst, ***Ind. Eng. Chem. Res.***, **2003**, ***42*** (2), pp 306–310

[34] Hamdy Farag, D. D. Whitehurst, and Isao Mochida, Synthesis of Active Hydrodesulfurization Carbon-Supported Co−Mo Catalysts. Relationships between Preparation Methods and Activity/Selectivity, Ind. Eng. Chem. Res. 1998, 37, 3533-3539

[35] Hamdy Farag, Kinetic Analysis of the Hydrodesulfurization of Dibenzothiophene: Approach Solution to the Reaction Network, *Energy & Fuels* 2006, *20*, 1815-1821

[36] M Daage, R . R Chainelli, Structure- Function relations in Molybdenum Sulfide Catalysts: "The Rim-Edge" Model. Journal of Catalysis 1994, 149, 414-427.

Vitae

Name	:Abdullah Faisal Abdullah Al-Ahmadi
Nationality	:Saudi
Date of Birth	:4/30/1984
Email	:afahmadi@kfupm.edu.sa
Address	:KFUPM P.O.Box 1951 Postal code 31261
Academic Background	:January ,2007 , BS in Chemistry from King Fahd University of Petroleum & Minerals
	May 2013, MS in BS in Chemistry from King Fahd University of Petroleum & Minerals